The Vif protein of maedi-visna virus

Protein interaction and new roles

Aðalbjörg Aðalbjörnsdóttir

Thesis for the degree of Master of Science
University of Iceland
Faculty of medicine
School of Health Sciences

HÁSKÓLI ÍSLANDS

Vif prótein mæði-visnuveiru

Prótein tengsl og ný hlutverk

Aðalbjörg Aðalbjörnsdóttir

Ritgerð til meistaragráðu í Líf og læknavísindum

Umsjónarkennari: Valgerður Andrésdóttir

Meistaranámsnefnd: Stefán Ragnar Jónsson og Ólafur S. Andrésson

Læknadeild

Heilbrigðisvísindasvið Háskóla Íslands

Júní 2016

The Vif protein of maedi-visna virus

Protein interaction and new roles

Aðalbjörg Aðalbjörnsdóttir

Thesis for the degree of Master of Science

Supervisor: Valgerður Andrésdóttir

Masters committee: Stefán Ragnar Jónsson and Ólafur S. Andrésson

Faculty of Medicine

School of Health Sciences

June 2016

Prentun: Háskólaprent

Reykjavík, Ísland 2016

Ágrip

Mæði-visnuveira (MVV) er lentiveira af ættkvísl retróveira. Hún veldur hæggengri lungnabólgu (mæði) og heilabólgu (visnu) í kindum. Aðalmarkfrumur veirunnar eru mónocytar/makrófagar. Veiran er náskyld HIV og hefur verið notuð sem módel fyrir HIV sýkingar.

Stöðug vopnakapphlaup milli veira og fruma hafa leitt af sér fjölda sértækra aðferða í vörnum hýsilsfrumu gegn veirusýkingum. Fruman hefur þróað með sér innrænar varnir gegn ýmsum sýkingum. Þessar varnir geta verið mjög sérhæfðar og tjáning þeirra spilar stórt hlutverk í hvaða frumur er hægt að sýkja og hverjar ekki. Dæmi um slíkan frumubundinn þátt eru APOBEC3 próteinin. APOBEC3 próteinin eru fjölskylda cytósín deaminasa sem geta hindrað retróveirur og retróstökkla. Þetta gera þau með því að afaminera cýtósín í úrasil í einþátta DNA á meðan á víxlritun stendur og valda þar með G-A stökkbreytingum í forveirunni. Vif (e. Virion infectivity factor) prótein lentiveira nýtir aftur á móti ubiquitin kerfi frumunnar til að ubiquitinera APOBEC3 og færa það til niðurbrots í proteasómi. Vif prótein HIV og SIV þurfa hjálp frá umritunarþættinum CBFβ til að starfa eðlilega en umritunarþátturinn reyndist hins vegar ekki nauðsynlegur fyrir virkni Vif próteina FIV, BIV og MVV. Komið hefur í ljós að Cyclophilin A (CypA) tengist Vif próteini MVV á tveimur stöðum um amínósýrurnar P21/P24 og P192.

Rannsóknir okkar sýna að með því að koma í veg fyrir bindingu CypA og Vif má endurheimta APOBEC3 virkni. Veira með stökkbreytingarnar P21A og P24A eftirmyndaðist hægar en villigerðarveira og hægar en veirur með hvora stökkbreytingu um sig. Einnig var tíðni G-A stökkbreytinga í P21A/P24A veirunni hækkuð. Veiru afbrigði sem inniheldur allar stökkbreytingarnar P21A/P24A/P192A eftirmyndast á svipuðum hraða og veira sem ekki getur bundið ubiquitin lígasann (SLQ-AAA) og er fjöldi APOBEC3 stökkbreytinga einnig sambærilegur. Aukin tíðni G-A stökkbreytinga er merki um APOBEC3 virkni og benda niðurstöðurnar til að Cyclophilin A hafi hlutverk í niðurbroti APOBEC3.

Auk próteasómsins, eru prótein einnig brotin niður í leysikornum í gegnum sjálfsát. Sjálfsáti hefur nýlega verið lýst sem mikilvægu ferli í ónæmissvari og hefur stýring á sjálfsáti verið tengd við ýmsar veirusýkingar, þar á meðal í HIV.

Niðurstöður okkar benda til að MVV hafi áhrif á sjálfsát við sýkingu. Makrófagar úr kindum sem sýktir hafa verið með MVV sýna tímabundna breytingu á sjálfsáti á þriðja og fjórða degi sýkingar. Þessi breyting er að einhverju leyti Vif háð, þar sem veira án Vif sýnir ekki sömu áhrif, en niðurstöður okkar sýna einnig að Vif prótein MVV bindur LC3 prótein í sjálfsátskerfinu. Þessar niðurstöður sýna nýja og áður óþekkta virkni MVV Vif.

Abstract

Maedi-visnavirus (MVV) is a lentivirus from the genus *retroviridae*. It causes a slowly progressing chronic pneumonitis (maedi) and encephalitis (visna) in sheep. Primary target cells of MVV are monocytes/macrophages. The virus is closely related to HIV and has been used as a model for HIV infection.

The constant arms race between virus and host has led to a number of specific approaches in the host cell defense against viral infections. The cell has developed internal defenses against various infections. These defenses can be highly specialized and their expression plays a big role in the permissiveness of cells. An example of this system are the APOBEC3 proteins which are a family of cytosine deaminases capable of inhibiting retroviruses and retrotransposons. They do so by the deamination of cytosine into uracil in single stranded DNA during reverse transcription, thereby causing G to A hypermutation in the provirus. The viral counterattack is mediated by the Vif protein (Virion infectivity factor) which hijacks the cell's ubiquitin system and utilizes it to mark APOBEC3 for degradation via the proteasome pathway. The Vif proteins of HIV and SIV need the transcription factor CBFβ for normal operation; however, CBFβ is dispensable for the activity of FIV, BIV and maedi-visna virus (MVV) Vif proteins. Recently Cyclophilin A (CypA) was found to act as a cofactor in MVV showing high affinity for three proline residues at P21, P24 and P192 on MVV Vif.

As a part of this study, the connection between (CypA) and MVV Vif was examined. The results show that point mutations in the aforementioned proline residues individually affected replication of the virus somewhat without G-A hypermutation, but a Vif P21A/P24A mutant replicated considerably slower than a wild type virus with significant increase in G-A mutations, and the triple mutant Vif P21A/P24A/P192A was even more attenuated, showing about the same amount of APOBEC3 activity as a MVV mutant unable to bind the ubiquitin ligase complex (SLQ-AAA). The results show that Cyclophilin A has a role in degrading APOBEC3 and is necessary for the correct function of MVV Vif.

Aside from the proteasome pathway, degradation of proteins also takes place in the lysosome through autophagy. Autophagy has recently been described as an important process in the immune response and modulation of the system has been associated with a number of viral infections, such as HIV.

Our research indicates that MVV modulates autophagy during infection. Primary macrophages from sheep infected with MVV show a temporary change in autophagy on the third and fourth day of infection. This modulation appears to be Vif mediated as a virus without v*if* does not show the same effect. In addition, MVV Vif protein binds to the LC3 protein, a key player in the autophagy system. These findings indicate a new and previously unknown function of MVV Vif.

Acknowledgments

I would like to thank my supervisors Stefán Ragnar Jónsson and Valgerður Andrésdóttir sincerely for all their patience, help and support during this project. I would also like to thank the third member of my M.Sc. Committee Ólafur S. Andrésson for his advice and help with this thesis. I would like to thank my fellow master student Katrín Möller for her help with western blotting techniques and confocal imaging and her supervisor Margrét Helga Ögmundsdóttir for invaluable input to this work. I am grateful to the administration at the Institute for Experimental Pathology, University of Iceland, Keldur where this research was carried out. I would like to thank all fellow students and co-workers at both Keldur and the biomedical center for their valuable advice and assistance at times of need. I would also like to thank my boyfriend Guðmundur F. Hallgrímsson for expert technical assistance as well as great support during this work. Finally I would like to thank all my family and friends for their understanding and encouragement through this process. The project was financially supported by the Icelandic Research Fund, Rannís.

Table of contents

List of figures

List of tables

Abbreviations

AIDS	Acquired immune deficiency syndrome
A3	APOBEC3
A3G	APOBEC3G
aa	amino acid
APOBEC3	Apolipoprotein B messenger RNA-editing enzyme catalytic polypeptide-like 3
BIV	Bovine immunodeficiency virus
CAEV	Caprine arthritis encephalitis virus
cDNA	Complementary DNA
CRL	E3-cullin-RING ubiquitin ligase
CypA	Chyclophilin A
DNA	Deoxyribonucleic acid
ds	Double stranded
EIAV	Equine Infectious Anemia Virus
Env	Envelope
FIV	Feline immunodeficiency virus
FOS	Fetal ovine synovial
Gag	*G*roup specific antigen
HEK293T	Human embryonic kidney 293T
Hs	Homo sapiens
LC3B	microtubule-associated protein 1 light chain 3 beta
LTR	Long terminal repeat
MOI	Multiplicity of infection
mTOR	Mammalian target of rapamycin
Nef	Negative Regulatory Factor
Oa	Ovies aries
PI3K	phosphatidylinositol 3-kinase
PIC	protease inhibitor cocktail
Pol	Polymerase
PPIase	peptidyl prolyl isomerase
PPT	Polypurine tract
PVDF	Polyvinylidene fluoride
Rev	Regulator of expression of virion proteins
RNA	Ribonucleic acid

RRE	Rev response element
RT	Reverse transcriptase
SCP	Sheep choroid plexus
S.D.	Standard deviation
S.E.M	Standard error of the mean
SDS-PAGE	Sodium dodecyl sulfate polyacrylamide gel electrophoresis
SIV	Simian immunodeficiency virus
ss	Single stranded
TAR	Trans-activating response element
Tat	Trans-Activator of Transcription
TFEB	Transcription factor EB
Vif	Virion infectivity factor
Vpr	Viral Protein R
Vpu	Viral Protein U
Vpx	Viral Protein X
WT	Wild type

1 Introduction

1.1 History of maedi-visna virus

The Icelandic words maedi and visna translate as shortness of breath and wasting, respectively. They describe the primary clinical signs displayed by the maedi-visna virus.

The maedi-visna virus (MVV) is a viral disease that causes slowly progressing chronic pneumonia and encephalitis in Icelandic sheep. The disease was previously described in other countries, such as ovine progressive pneumonia in the US, but was first studied in Iceland. The virus was unintentionally brought to Iceland in 1933 with 20 sheep of the Karakul breed imported from Germany. They were to be used as an economical booster as Icelanders wished to start production of fine Persian lamb skins. The healthy Karakul sheep were quarantined for two months before being distributed to 14 farms around Iceland. In 1935 the first cases of two new diseases started to emerge, clinical signs were weight loss and shortness of breath with breathing gradually becoming very difficult eventually leading to death(Sigurdsson et al., 1952). This disease was called maedi. The other was a disease of the central nervous system seen amongst maedi infected stock. First signs of disease were sometimes an unnatural position of the head, mild ataxia and partial paralysis, particularly of the hind legs. The disease would progress into full paralysis and eventually death, this was called visna (Sigurdsson et al., 1957). With both diseases, symptoms would worsen over the course of a few weeks to several months and were only observed in adult sheep 2 years or older. Transmission was mostly by inhalation of virus as sheep are housed together during winter. Further studies of the diseases showed that they were caused by filterable viruses with a very long incubation period. Maedi and visna virus particles proved very similar viewed with an electron microscope, with viruses causing similar cytopathic changes in cell cultures. Further experiments in vivo where flocks of sheep were infected with one virus but would show signs of both diseases led to the conclusion that maedi and visna were caused by a strain of the same viral species, leading to the name maedi-visna virus(Gudnadottir & Palsson, 1967; Thormar, 2005, 2013).

Icelandic sheep proved especially susceptible to the previously unknown virus probably due to evolutionary and geographical isolation. Interestingly maedi is the typical disease form found with MVV infection whereas visna has rarely been described outside Iceland. An eradication program of maedi infected flocks proved successful with Iceland being the only country in the world to have successfully eradicated MVV from livestock (Thormar, 2005, 2013). Paratuberculosis, a bacterial disease that also came with the Karakul sheep, has yet to be eradicated (Fridriksdottir et al., 2000).

1.2 Retroviruses

In the Baltimore classification system of viruses, viruses are organized based on their nucleic acid genome, be it DNA or RNA, single (ss) or double stranded (ds), circular or linear and how viral mRNA is produced in permissive cells. According to this system retroviruses are located in group VI containing positive sense ssRNA, with two linear copies of the genome per virus particle (Ward et al., 2009). All retrovirus genomes include the genes *gag* (group specific antigen)*, pol* (polymerase), and *env* (envelope).

The retrovirus family is divided into two subfamilies, *orthoretrovirinae* and *spumaretrovirinae*. *Orthoretrovirinae* contains the genera of Alpha, Beta, Gamma, Epsilon, Delta and lentiviruses whereas *spumaretrovirinae* only contains spumaviruses. The retrovirus family can also be divided based on genomic complexity into the simple Alpha, Beta, Gamma, Epsilon, and the complex Delta, Spuma and Lentiviruses, where lentiviruses are the most complex, containing up to 6 extra genes in addition to the common retrovirus genes *gag*, *pol*, and *env*. Taxonomy is based mostly on Phylogenetic analysis of the *pol* gene (figure 1) (Coffin et al., 1997; Weiss, 2006). A noteworthy characteristic of retroviruses is the inclusion of reverse transcriptase (RT) in the viral particle. RT is an RNA dependent DNA polymerase that produces complimentary cDNA from the viral RNA genome.

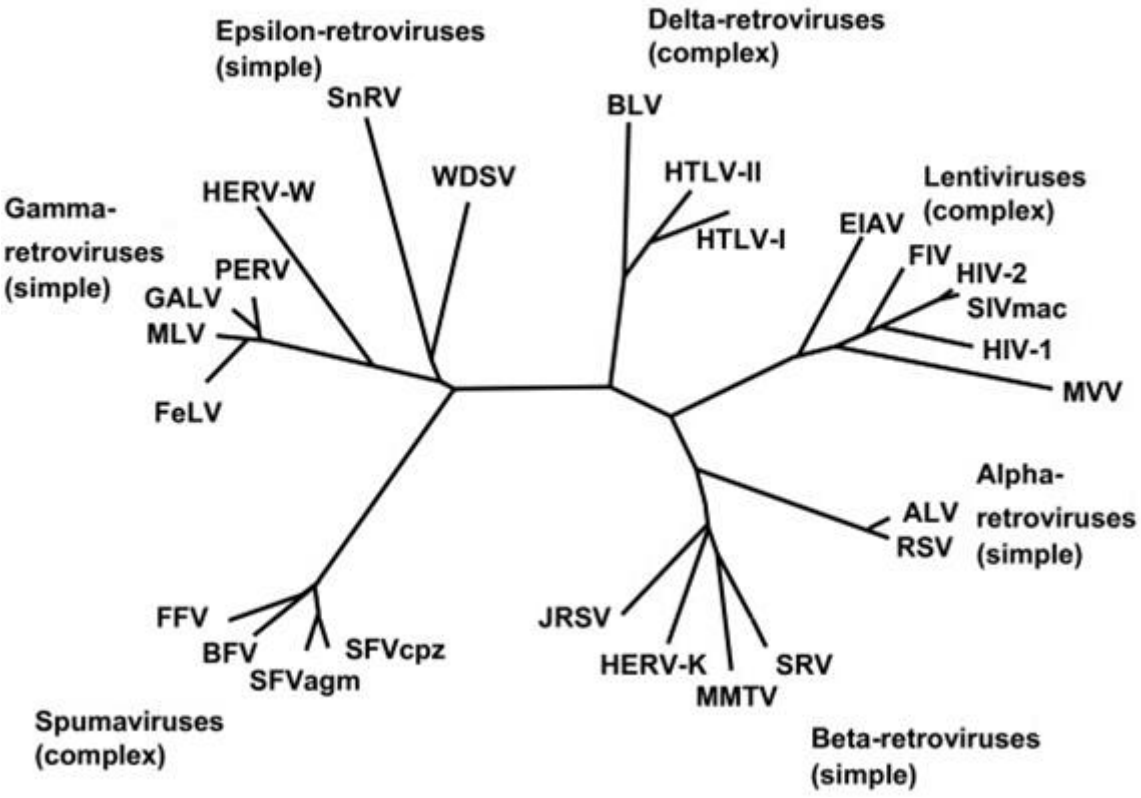

Figure 1 Phylogenetic tree of retroviruses. (Weiss, 2006).

1.3 Lentiviruses

The name lentivirus is taken from the latin word “lentus” meaning slow. As the name indicates these viruses cause a slowly progressing disease in its host and is found in many mammals. To date lentiviruses have been described in sheep (MVV), goats (Caprine arthritis encephalitis virus, CAEV), cows (Bovine immunodeficiency virus, BIV), horses (Equine Infectious Anemia Virus, EIAV), cats (Feline immunodeficiency virus, FIV), humans, (Human immunodeficiency virus, HIV-1 and HIV-2) and several in other primates (simian immunodeficiency viruses, SIVs) (Gonda, 1994). FIV, HIV and SIV infect both T-lymphocytes and macrophages, however BIV, CAEV, EIAV and MVV infect mainly macrophages.

During the classification of HIV a strong correlation between HIV and MVV supported the inclusion of HIV in the lentivirus subfamily (Sonigo et al., 1985).

As mentioned in section 1.2, lentiviruses are the most complex of all retroviruses. They contain the genes common to all retroviruses but also multiple splice donors in the genome that allow for greater diversity of gene products. The regulatory gene *rev* is common to all lentiviruses, and EIAV, SIV and HIV harbor the regulatory gene *tat*. Accessory proteins found in some but not all lentiviruses include Vif (Virion infectivity factor), Vpr (Viral Protein R), Nef (Negative Regulatory Factor), Vpu (Viral Protein U), Vpx (Viral Protein X) and a dUTPase.

Vif can be found in all lentiviruses except EIAV. Primate lentiviruses include Vpr and Nef. A gene in MVV called tat is related to vpr. Additionally, HIV-1 and SIVcpz have Vpu whereas HIV-2 and most other SIV viruses contain Vpx. All non-primate lentiviruses have a dUTPase included in their *pol* gene (Sonigo et al., 1985).

The overall genome organization is quite conserved between all retroviruses. On each end of the genome is an LTR (long terminal repeat) sequence critical for reverse transcription, transcription regulation and integration of the provirus. The LTR is divided into U3(unique), R(repeat) and U5, further discussed in 1.1.4 (Shors, 2011). Comparison of the HIV and MVV genome can be viewed in figure 2.

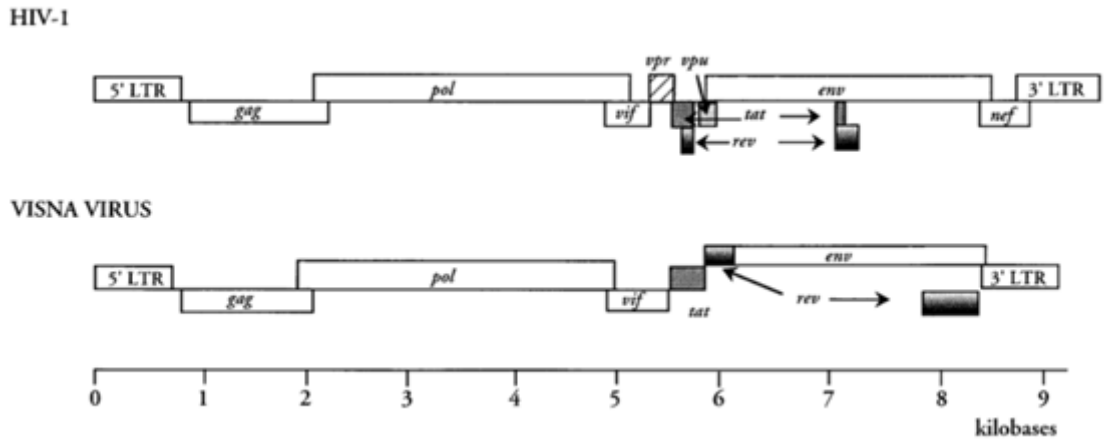

Figure 2 Genome of HIV-1 compared with MVV. General organization of genes is conserved between lentiviruses (Clements & Zink, 1996)

The *gag* gene stores information for the core structural proteins matrix (MA), capsid (CA) and nucleocapsid (NC). The matrix protein forms a shell under the virus membrane. It is 15-20 kDa. The capsid protein is as the name indicates the major structural protein of the viral capsid, its size is 24-30 kDa. Nucleocapsid proteins are 10-15 kDa and are found around the viral genome. Its high affinity for RNA binding is due to zinc-finger domain that recognizes specific loops on the ssRNA (Allen et al., 1996; Coffin et al., 1997; De Guzman et al., 1998). Frameshifting allows for a Gag-Pol poly protein to be formed in 5-10% of unspliced mRNA, this happens when ribosomes jump back one nucleotide at the 3' end of

gag bypassing the 3´end stop codon of *gag*. Then continue into the *pol* reading frame (Acheampong et al., 2003).

The *pol* gene codes for reverse transcriptase (RT), integrase (IN) and protease (PR). The RT enzyme is responsible for reverse transcription after a virus particle infects a new cell. The RT has both polymerase activity, transcribing RNA to DNA during reverse transcription, as well as RNase H activity that degrades the viral RNA genome during reverse transcription. The IN proteins aid the integration of the provirus into the host cells genome. They have endonuclease activity that cleaves two nucleotides of each of the 3´ ends on the provirus then helps integration at random sites into the host cells genome. This step is irreversible and establishes a permanent source of virus in the host. The PR proteins form a dimer out of two subunits. The PR protein is the viruses very own protease that cleaves the viral polyproteins after budding, promoting virus particle maturation. The active site has two aspartic acid from each monomer creating a highly acidic environment for proteolytic activity. The *pol* gene also encodes for a dUTPase in non-primate lentiviruses. dUTPases turn dUTP into dUMP and diphosphate, this function decreases uracil content in nucleotide pools. This process helps keep DNA clear of unnecessary uracils and in that sense facilitates correct DNA replication (Coffin et al., 1997; Sundquist & Kräusslich, 2012).

The env gene codes for the envelope proteins surface (SU) and transmembrane (TM). The size of these proteins varies within the retrovirus family. The Env polyproteins are post translationally modified in the Golgi system by addition of oligosaccharides, necessary for correct folding of the proteins. There they are also cleaved into the SU and TM subunits by cellular proteases. Aside from forming the viral envelope these proteins additionally contain sites for viral binding and are the reason for membrane fusion. Because these proteins bind to cell receptors they also control what cells the virus can infect. The viral Gag polyprotein promotes the assembly of the virus particle, recruiting and concentrating Env proteins (Coffin et al., 1997; Sundquist & Kräusslich, 2012).

1.1.1.1 Tat and *Rev*

The trans-activator of transcription (Tat) and the regulator of expression of virion proteins (Rev) control gene expression of the integrated provirus. Rev is about 20 kDa in HIV and identified as a phosphoprotein. It has both a nuclear localization and nuclear export signal, allowing it to travel in and out of the nucleus exporting viral mRNAs (Cochrane et al., 1989). Tat is 14 kDa in HIV-1, a transcription factor that binds Trans-activating response element (TAR), and recruits proteins responsible for polymerase II regulation (Bagashev & Sawaya, 2013; Karn & Stoltzfus, 2012).

1.1.1.2 Vif

The MVV Vif protein is 29 kDa in size and 230 amino acids. The Vif protein of HIV is smaller 23kDa and 192 amino acids. The accessory *Vif* gene can be found in all lentiviruses except EIAV (figure 3). They differ in size and amino acid sequence except for a conserved T/SLQXLA (where X can be any amino acid) on the C-terminal end. This sequence is necessary for APOBEC3 degradation. The HIV-1 Vif

protein is known to contain a unique zinc-finger motif. Vif proteins of MVV and HIV are found in the cytoplasm and incorporated into budding virus particles.

Vif's function is to battle APOBEC3 activity, discussed further in 1.2.1 and 1.3.

The ΔVif phenotype allows the possibility of classifying cells based on whether they are permissive or non-permissive to the virus mutant. Macrophages and sheep choroid plexus cells (SCP) are both non-permissive, macrophages are natural targets of the virus whereas SCP cells are utilized in the lab. Vif is necessary for proper virus replication in non-permissive cells and also for in vivo infections. High levels of G-A mutations are found in non-permissive cells (Kristbjornsdottir et al., 2004; von Schwedler et al., 1993).

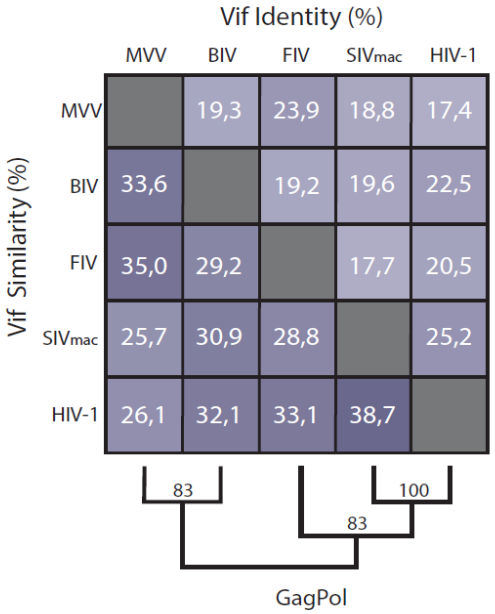

Figure 3 Vif percentage similarity between lentiviruses. Shows the percentage similarity and identity between different virus types. Although the Vif proteins all have the same function they don't share more than 25% sequence identity. The distance tree was generated from Gagpol protein sequence of viruses, with bootstrap support values (Kane et al., 2015).

Vif's role was elusive for a long time and whether it has other roles than APOBEC3 degradation has yet to be determined. Previous experiments performed at Keldur describe the phenotype of the CA-Vif double mutant. The combination of single amino acid substitution in the CA protein (L121R) and another mutation in Vif (P205S) cripples virus replication in both macrophages and FOS cells but not SCP cells. Each mutation on its own is not enough for this effect. No G-A mutations are found in this virus type indicating that APOBEC3 activity is not the reason for low replication rates. This implies a new undiscovered function of Vif (Gudmundsson et al., 2005).

The HIV-1 Vif protein structure has proved difficult to capture with crystallography. The only available crystal structure is in complex with other proteins of the CRL complex, Cullin 5, ELOB and ELOC and CBF-β (Guo et al., 2014). Two partial crystal structures are also available (Lu et al., 2013; Stanley et al., 2008). Figure 4 shows the crystal structure of HIV-1 Vif from Guo et al. excluding other proteins. The Vif of HIV-1 has been shown to have a rather short half-life of about 3 minutes and be degraded by cellular proteasomes (Akari et al., 2004).

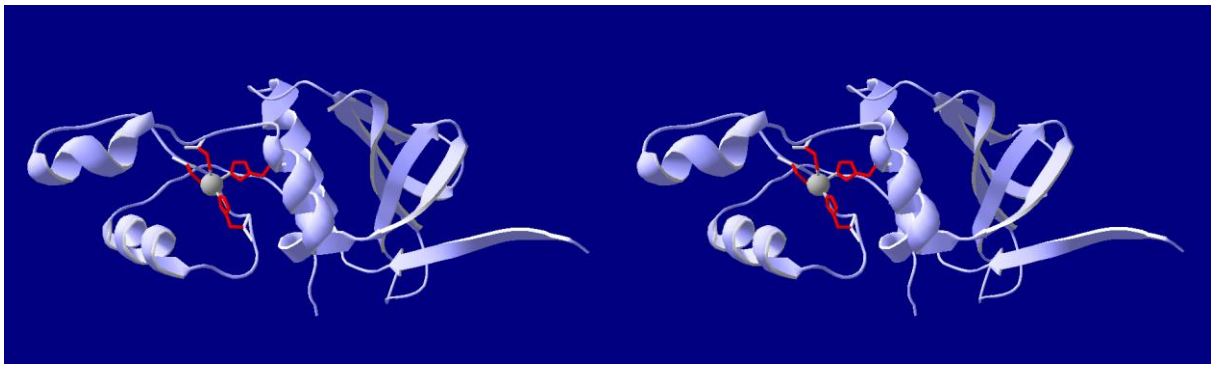

Figure 4 Crystal structure of Vif from PDB: 4N9F. Stereo view of HIV-1 Vif showing HIS108, CYS114, CYS133 and HIS139 in red binding Zn^{2+} ion colored in grey (Guo et al., 2014).

1.1.1.3 HIV proteins connected to autophagy modulation

Modulation of autophagy has been shown to be an important step for many viruses (Dong & Levine, 2013; Lin et al., 2010; Shintani & Klionsky, 2004; Sir & Ou, 2010). It has been demonstrated that HIV modulates autophagy during infection to promote its own replication, first by increasing it and then by inhibiting autophagy (Campbell & Spector, 2013). The Gag protein seems to hitchhike on autophagosomes in its early nondegradative stages, perhaps as a means of transport but also to complete its maturation (Kyei et al., 2009). The Nef proteins are a key players in autophagy inhibition by binding Beclin 1, which activates mTOR (mammalian target of rapamycin) and mediates transcription factor EB (TFEB) phosphorylation and therefore its retention in the cytoplasm (Campbell et al., 2015). A new study has further shown that HIV Vif interacts with LC3 and inhibits autophagy in CD4+ T cells (Borel et al., 2015).

1.1.2 Structure

The MVV particle is about 100 nm in diameter. It has a lipid bilayer that the virus gains when budding from an infected cell. On and through the membrane are two surface (SU) and trans-membrane (TM) glycoproteins. Matrix proteins (MA) form a frame under the membrane and in the core of the virus is the cone shaped capsid (CA) that incases the viral genome and core proteins. Inside the capsid nucleocapsid (NC) proteins bind the viral ssRNA and cellular $tRNA^{lys}$ which the virus uses as a primer during reverse transcription. Other proteins are; protease (PR) that cleaves gag-polyproteins during virus maturation, reverse transcriptase (RT) necessary for reverse transcription of the virus RNA after fusion with a susceptible cell and integrase (IN) facilitates the integration of provirus into the host cell's DNA. Accessory proteins are also found in the mature virus such as Vif in MVV that hinders APOBEC3 activity in permissive cells (Shors, 2011; Thormar & Cruickshank, 1965). Figure 5 shows the general structure of a mature virus.

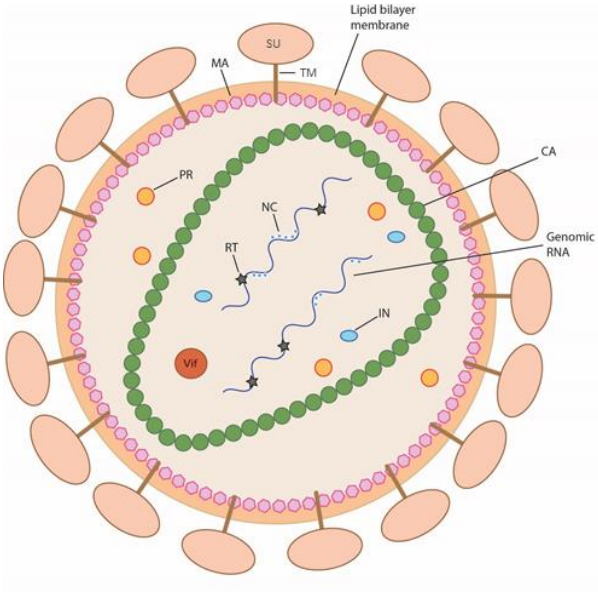

Figure 5 Lentivirus structure. A simplified version of the virus particle showing the conformation of the viral proteins.

1.1.3 Replication

Since MVV replication has not been studied in as much detail as HIV, HIV will serve as a model for the replication cycle in lentiviruses.

First receptor binding of viral glycoproteins and cellular receptors facilitate the fusion of the viral membrane with the cells, for HIV these proteins are SU glycoprotein on the virus and CD4 receptor on the cell. HIV also needs a co-receptor, CXCR4 in T-lymphocytes and CCR5 in macrophages. Binding to these receptors causes conformational changes in TM glycoprotein that starts the fusion of the two membranes exposing the viral capsid into the cytoplasm (Malashkevich et al., 2001). MVVs receptor is still unknown, however MVV ability to enter cells of many types from many species indicates the receptor is a common surface molecule (Lyall et al., 2000).

Uncoating of the viral capsid takes place and reverse transcription starts, explained in detail in 1.1.4. In HIV-1, IN along with MA, RT and Vpr form a preintegration complex (PIC) with the proviral DNA, this complex promotes the integration of the provirus into the host cell's genome. Using the cells own transcription proteins, new viral proteins can be synthesized. Transcription starts at intersection of U3 and R at the 5' end of the provirus. The first transcripts are for Rev and Tat, Rev is necessary to guarantee un- or single spliced out of the nucleus. Fully spliced Tat and Rev transcripts are exported out of the nucleus and when levels of Rev become high enough, Rev binds to the Rev response element

(RRE) which is found on all un- or partially spliced RNA transcripts, stopping further splicing and promoting transport out of the nucleus. RNA transcripts have a 5´methyl cap and a polyA tail in U3 on the 3´end. By binding to TAR, Tat increases the basal transcription level up to thousand fold. MVVs basal transcription level is about 50 times higher than in HIV-1 and the role of Tat in MVV is more similar to the role of Vpr in HIV-1 (Villet et al., 2003). The accessory proteins Vif, Vpr and Vpu and other full length unspliced transcripts such as the Viral genomic RNA and mRNAs for Gag and Pol can now be synthesized (Acheampong et al., 2003; Freed, 2001).

As with cellular mRNA transcripts, translation of viral mRNA is performed in polyribosomes and released into the cytoplasm or the endoplasmic reticulum (ER). Gag, Gag-pol and Env proteins gather by the cell membrane. Gag proteins form a coat on the inner side of the membrane and Env proteins SU and TM are found in the cell membrane. The N-terminal end of the Gag polyprotein is myristoylated allowing for strong association between Gag and the cell membrane (Li et al., 2007). Unspliced transcriptional products of the *gag* gene give in 5-10% of the time a Gag-Pol polyprotein due to frameshifting. This frameshift event secures the expression of the Pol proteins; IN, PR, RT and dUTPase (in non-primate viruses) necessary for the virus particle.

Env precursor glycoproteins are trafficked through the ER, there they are cotranslationally glycosylated and inserted into the lumen. After translation is done the monomeric units form oligomers and travel from the ER to the Golgi system. Here host cell protease cleaves the glycoprotein forming the SU and the TM.

During budding, viral proteins, RNA and host factors are incorporated into the immature virus particle. After budding the viral PR cleaves Gag and Gag-Pol polyproteins that are now capable of forming the fully mature virus particle. Maturation is essential for virus infectivity (Acheampong et al., 2003; Freed, 2001; Shors, 2011; Sundquist & Kräusslich, 2012).

A schematic diagram of viral replication can be viewed in figure 6. The figure also shows possible host cell restriction factors and viral counter measures that are further discussed in 1.2.

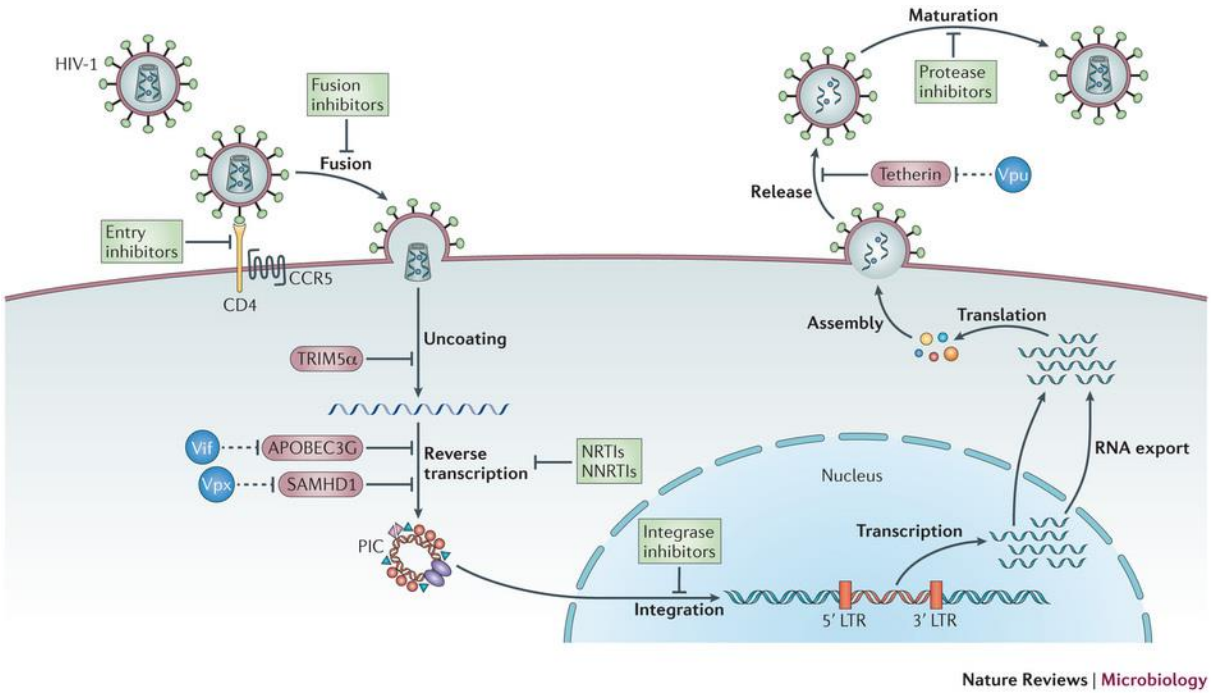

Figure 6 Replication of HIV including restriction factors. The general process of viral replication from entry to virus maturation, including host cell restriction factors (purple) and viral counter measures (blue) as well as possible antiviral drug treatments (green) Reprinted by permission from Macmillan Publishers Ltd: [Nature Reviews Microbiology] (Barre-Sinoussi et al., 2013), copyright (2013).

1.1.4 Reverse transcription

As mentioned before each virus particle includes two copies of a + ssRNA genome. Synthesis of viral DNA by RT is initiated by the 5´ end of the RNA using a host $tRNA^{lys}$ that anneals to the primer binding site. The process of reverse transcription can best be understood with representational graphics such as the one in figure 7 from (Katz & Skalka, 1994; Sarafianos et al., 2009). The steps of reverse transcription are as follows:

1. From the tRNA primer, DNA is synthesized through the U5 region ending at the R region, this is referred to as the minus-strand strong stop DNA.
2. RNase H activity of the RT digests the viral RNA of the RNA – DNA mixed strand, exposing a ssDNA product.
3. Exposure of the ssDNA makes binding to the R region of the 3´ end possible. This can be inter- or intra-molecular. This step is also known as the first jump.
4. Minus strand elongation continues. RNase H cleavage at the border of a region known as the polypurine tract (PPT) forms a unique plus-strand RNA primer from where the plus DNA strand can be synthesized back to the U5 region now using the minus DNA strand as template.
5. Minus strand DNA synthesis continues through the whole genome and RNase H activity erases the RNA template.
6. More RNase H digestion products are thought to serve as additional primers for plus strand synthesis.

7. A step known as the plus strand strong stop is when the plus strand synthesis reaches the PBS. The tRNA primer is removed by RNase H revealing ssDNA on the plus strand end.
8. The second jump is when the PBS on the plus and minus strand anneal to one another always intra molecular making a closed circle.
9. The finished linear dsDNA product with LTRs at both ends is formed either by strand displacement synthesis by RT from the PBS and PPT ends, and/or repair and ligation of the circular intermediate.

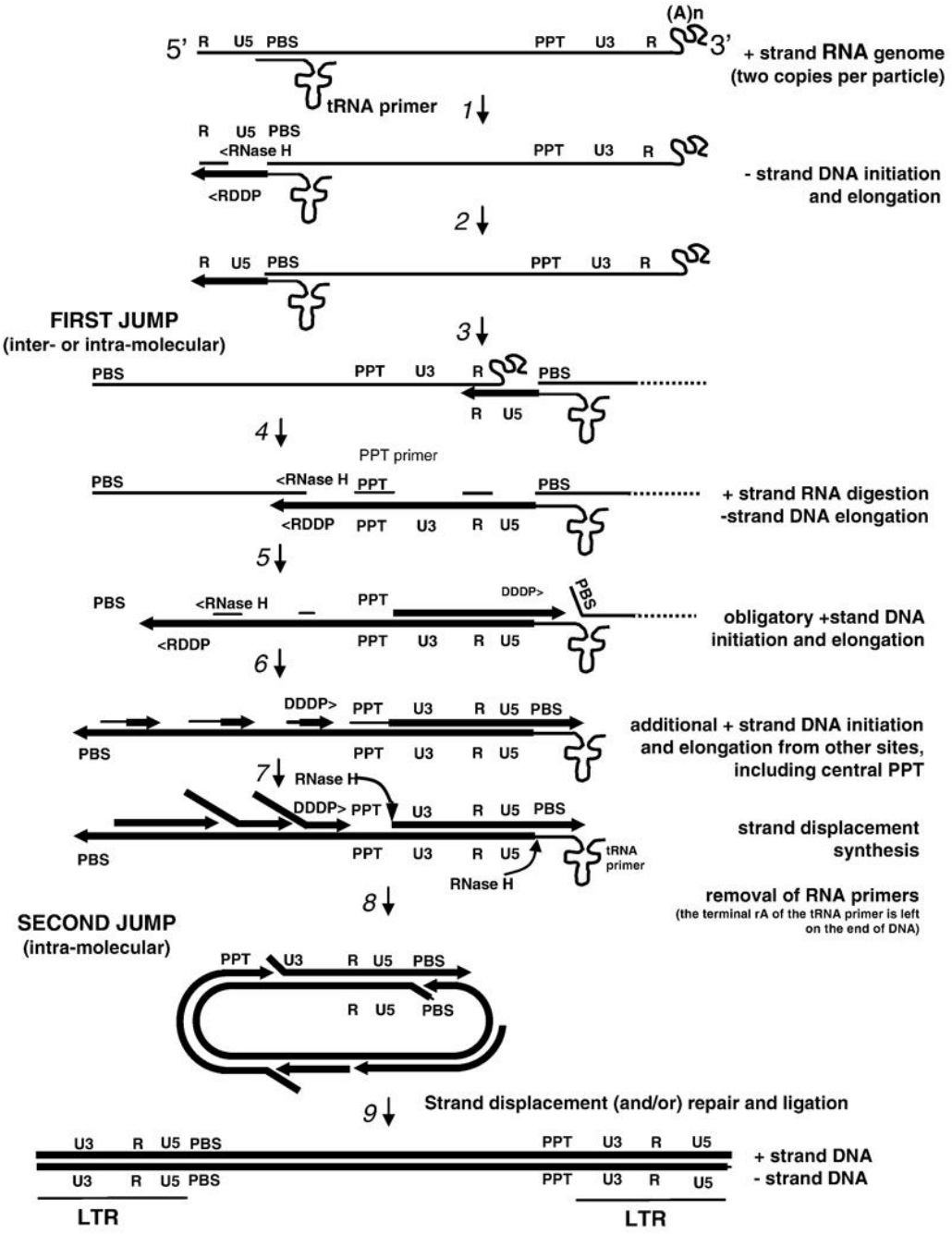

Figure 7 Reverse transcription. (Katz & Skalka, 1994).

1.2 Retroviral host defense in mammals

As described in Figure 6, a number of host cell restriction factors are already known. Since lentiviruses have the ability to evolve very quickly they have developed their own countermeasures to evade these factors. Research into restriction factors hopes to gain some insight into how viruses infect cells and why some cells are more permissive than others, additional goals are to find new ways to combat viral infections with development of new anti-virals based on new targets.

The most studied factors are APOBEC3G (A3G), SAMHID1 and tetherin. Their viral counteragents are Vif, Vpx and Vpu respectively. Another well studied restriction factor is TRIM5α that has no known counteragent (Malim & Bieniasz, 2012).

1.2.1 The APOBEC3 proteins

The APOBEC3 proteins, also known as apolipoprotein B messenger RNA (mRNA)-editing enzyme catalytic polypeptide-like 3, are members of a family of vertebrate proteins that have cytidine deaminase activity. This allows them to post-synthesis modify RNA or DNA by changing cytidine residues to uridines. APOBEC proteins contain one or two Z domains containing the conserved sequence motif His-Xaa-Glu-Xaa_{23-28}-Pro-Cys-Xaa_{2-4}-Cys. Z domains can further be divided into three sub types Z1, Z2 and Z3 based on conserved amino acid residues aside from the previously mentioned motif. The Z domain is the active site of the protein containing a Zn2+ ion and catalytic glutamic acid residue. In duplicated proteins such as in the Human A3G protein, two Z domains are found but only the C-terminal domain mediates deamination. The N-terminal domain facilitates incorporation into virus particles and is recognized by HIV Vif.

In retrovirus infections the A3s cytidine deaminase activity generates mutations in the viral DNA, often leading to attenuated viruses. This viral DNA is either degraded or integrated without the ability to produce new virus particles. As much as 10% of cytidines will be edited producing characteristic guanosine-to-adenosine hypermutation in the viral plus strand (LaRue et al., 2009; Malim & Bieniasz, 2012). A3 will target specific sites for mutation. In MVV the first G of sequence containing GAA and GGA are eligible for mutation (Franzdottir et al., 2016; Jonsson et al., 2006). Restriction mechanism of APOBEC3 proteins together with Vif's countermeasure can be viewed in figure 8.

Humans encode seven A3 proteins, HsA3A, HsA3B, HsA3C, HsA3DE, HsA3F, HsA3G and HsA3H where Hs stands for *Homo sapiens*. They show different affinity against various retroviruses and retrotransposons. Sheep code for three A3 proteins A3Z1, A3Z2 and A3Z3 based on their conserved Z domain amino acid sequence producing four proteins, three single domain and one double. MVV Vif is able to almost completely degrade the OaA3Z2-Z3 double domain protein (LaRue et al., 2009; LaRue et al., 2010). As an example of APOBEC3s efficiency, the APOBEC3 proteins of mice, cows, sheep, pigs and cats can all block WT HIV-1 infections.

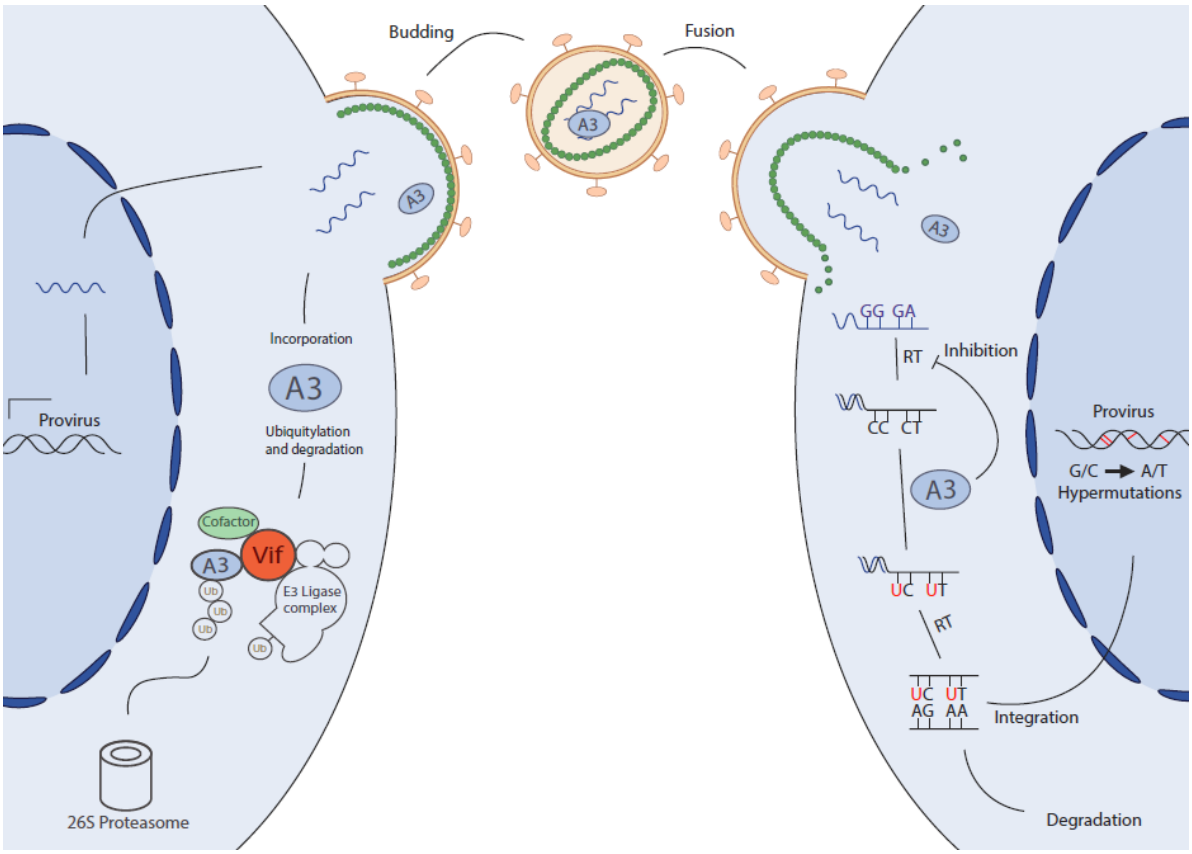

Figure 8 APOBEC3 in viral infection. If Vif is debilitated, permissive cells that produce A3 will incorporate the A3 into new virus particles. When these particles infect susceptible cells, A3 will deaminate cytidine residues in negative ssDNA. With a functional Vif A3 is marked for degradation via the ubiquitin proteasome pathway.

1.3 The ubiquitin-proteasome pathway

Eukaryotic cells have several different ways to dispose of and recycle old and defective cell proteins. The ubiquitin-proteasome pathway is one of them. Ubiquitin is a small 8,5 kDa protein made up of 76 amino acids. Ubiquitin can be used as a post translational modification of proteins but the number and order of the ubiquitin determine the protein substrates fate. Ubiquitin binds covalently to lysine side chains and will also bind lysine side chains of other ubiquitin proteins generating a poly-ubiquitin chain. Ubiquitin has seven highly conserved lysine residues; K6, K11, K27, K29, K33 K48 and K63 that are used in ubiquitin signaling. A chain with four K48 linked residues gives a signal for brake down via the proteasome pathway. Brake down is achieved using the 26S proteasome that consists of a 20S center with 19S units at each end. The 26S proteasome is found both in the nucleus and cytosol. Proteolysis is induced by ATP hydrolysis (Petroski & Deshaies, 2005).

Generally an ubiquitin activating enzyme, E1, binds the C-terminal end of the ubiquitin by ATP hydrolysis and then further catalyzes the transfer of the ubiquitin to E2, an ubiquitin conjugating enzyme. An E3 ubiquitin ligase will bind both the substrate and E2 then catalyze the attachment of ubiquitin from E2 to the substrate.

A SOCS-box domain helps in targeting proteins for ubiquitination through ECS-type (Elongin C-cullin-SOCS-box) E3 ubiquitin ligase family. These domains are found at the C-terminal end of many proteins. Involved with the SOCS-box is a domain called BC-box. The BC-box domain is very similar to the highly conserved SLQXLA sequence found in lentiviral Vifs. Vif also mimics the SOCS-box proteins by conformation rather than amino acid sequence (Stanley et al., 2008). Using this, Vif hijacks E3-cullin-RING ubiquitin ligase (CRL) binding to the Cullin protein. There are several variations of CRLs using different Cullin proteins. Vif of HIV is known to use Cullin 5 whereas the Vif of MVV uses either Cullin 2 or 5, possibly both. The possibility of Vif utilizing both but for different means has been hypothesized. For degradation of A3, Vif mediates the binding of ubiquitin to A3. To stabilize the complex a cofactor is needed in some but not all lentiviruses. The cofactor of HIV is CBFβ and for MVV it is Cyclophilin A (CypA) (figure 9) (Kane et al., 2015). Figure 9 shows how Vif binds several different proteins to achieve the ubiquitination of A3G.

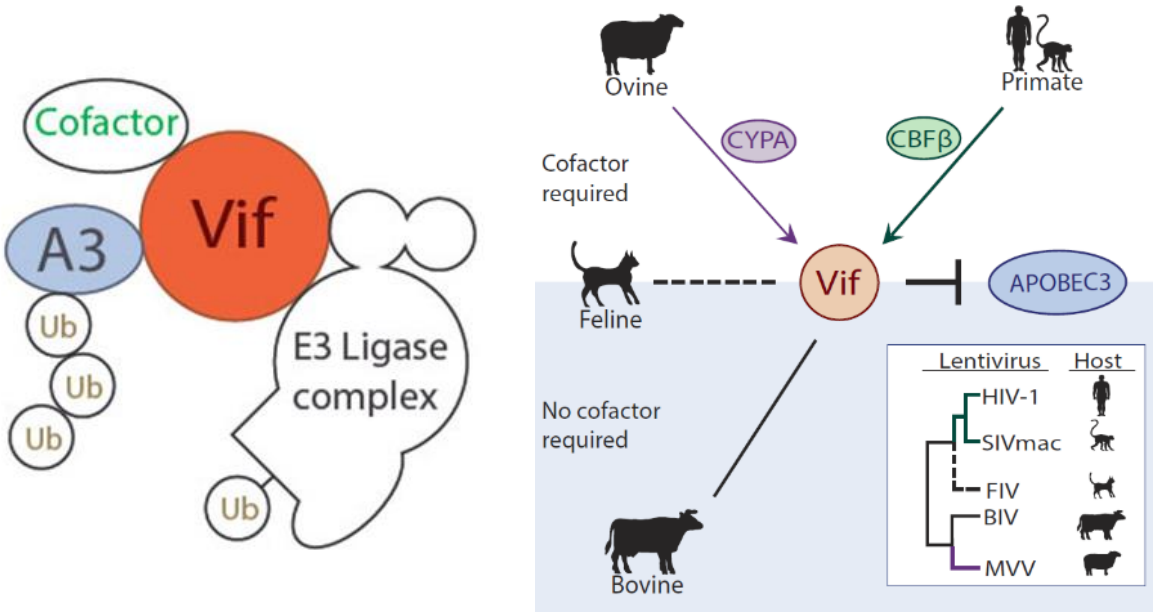

Figure 9 Vif, cofactors and the ubiquitin ligase complex. To the left diagram of Vif bound to E3 ligase complex, APOBEC3 and a cofactor. To the right Cofactors of Vif for A3 degradation. The primate viruses use CBFβ as a cofactor and the ovine virus uses CypA. The feline virus may use a cofactor that has yet to be identified and the bovine virus does not require a cofactor (Kane et al., 2015).

1.3.1 Cyclophilin A

Cyclophilin A (CypA) is an abundant cytosolic protein found in vertebrates, also known as peptidyl prolyl isomerase A. It has peptidyl prolyl isomerase (PPIase) activity that catalyzes the isomerization of peptide bonds from trans to cis, specifically at proline residues and in doing so facilitates correct protein folding. CypA is not only an intracellular protein that regulates proteins folding and trafficking but may also be secreted in response to inflammatory stimuli. CypA regulation has been connected to a number of diseases such as aging, asthma, cancer, cardiovascular diseases, diabetes, neurodegeneration and sepsis (Nigro et al., 2013; Obchoei et al., 2009). As mentioned in 1.3, Cyp A is needed to stabilize the ubiquitin complex with MVV Vif. It has also been shown to be recruited by the Gag polyprotein in HIV-1

infections and is incorporated in new virus particles. During maturation of the virus particle CypA relocates to the viral surface and is thought to help with capsid uncoating or viral infectivity perhaps by blocking TRIM5α. CypA-binding appears to stabilize or destabilize the HIV-1 capsid, depending on the cell type, and is thought to act at the time of reverse transcription, nuclear entry or integration. However, in non-human primate cells CypA interaction with CA enhances the anti-HIV-1 restriction activity of Trim5α (Liu et al., 2016). The interaction of CYPA with HIV-1 capsid has recently been found to be essential for the virus to evade detection by the innate immune sensor cGAS and to avoid subsequent activation of the innate immune response (Rasaiyaah et al., 2013). The MVV Gag polyproteins do not recruit CypA (Kane et al., 2015).

1.4 Autophagy

The term autophagy is derived from Greek and means “self-eating”. It is a way for the cell to manage waste products and recycle necessary building blocks independent of the proteasome pathway. This process is indispensable for cell homeostasis as it is a fundamental system for providing the cell with nutrients and energy when starved and also plays an important maintenance role in the degradation of damaged organelles and proteins. Autophagy is also known to target intracellular pathogens. Selection of material to be recycled is thought to be based on ubiquitination or acetylation. Several receptors have been identified that recognize and recruit ubiquitinated protein aggregates that will be degraded in the autophagy pathway (Glick et al., 2010).

Autophagy can be categorized into macroautophagy, microautophagy and chaperone-mediated autophagy. Macroautophagy is where cytoplasmic materials such as organelles and intracellular pathogens are destroyed by de novo formation of double-layer membranes. Microautophagy is used to describe the engulfment of a part of the cytoplasm by the invagination of lysosomal membrane into lysosome lumen. Chaperone-mediated autophagy is when specific cytosolic proteins are chaperoned to lysosome for degradation (Glick et al., 2010). Macroautophagy is a focus of this thesis and will hereafter be referred to as autophagy.

Deregulation of the autophagy system has been described in several diseases such as cancer, neurodegenerative disorders and immune diseases. It is also part of the intracellular immune response to intracellular pathogens, many viruses have however developed ways to fight this system and use it for their own replicative needs. Examples of such viruses are HIV-1, herpes simplex virus, hepatitis C virus, influenza virus and more (Dong & Levine, 2013; Lin et al., 2010). The HIV envelope protein expressed at the cell surface of infected cells is known to trigger autophagy in Bystander CD4+T cells that leads to their apoptosis. This effect is central to the development of immunodeficiency caused by HIV (Espert et al., 2006). Autophagy may also on its own be able to cause what is called autophagic cell death displayed by large-scale accumulation of autophagosomes before the death of the cell (Kroemer & Levine, 2008).

Autophagy is a strictly regulated process, involving at least 35 genes in humans. The transcription factor EB (TFEB) is central to this process. It is a basic helix-loop-helix leucine zipper that binds DNA. When cellular conditions are unfavorable, such as during starvation, cells activate a

transcriptional program coordinated by TFEB that controls all major steps of the autophagic pathway (Settembre et al., 2011). This response is mediated by the kinase mTOR, a conserved serine/threonine kinase. The class I phosphatidylinositol 3-kinase (PI3K)-Akt/PKB signaling pathway as well as high concentrations of amino acids are important activators of mTOR allowing formation of mTORC1 (mTOR complex 1). High AMP/ATP ratios and hypoxia however inactivate the PI(3)K pathway. When activated, mTORC1 phosphorylates Ser^{142} and Ser^{211} of TFEB at the lysosomal membrane, enabling it's binding to 14-3-3 in the cytosol and keeps it from nuclear entry. Upon starvation, mTOR is not active, resulting in unphosphorylated TFEB entering the nucleus (Campbell et al., 2015; Martina et al., 2014).

Beclin1 (ATG6) is another well-known key regulator of autophagy. It interacts with the class III PI(3)K. It is involved in autophagic vesicle nucleation, it recruits additional Atg proteins for autophagosome formation. Beclin1 has also other functions independent of autophagy and its deregulation is connected to a number of diseases (He & Levine, 2010; Wirawan et al., 2012).

Formation of the autophagosome needs two intertwined conjugation systems (figure 10). In a series of ubiquitin system like steps, Atg proteins elongate the phagophore memebrane (figure 10 (a)) and the cytosolic microtubule-associated protein 1 light chain 3 beta (LC3B)-I is converted to LC3B-II involving ATG7 and ATG3. The cytosolic form, LC3-I is conjugated to phosphatidylethanolamine to form LC3-phosphatidylethanolamine conjugate, or LC3-II (figure 10 (b)). ATG12–ATG5-ATG16L1 complex functions as an E3-like ubiquitin ligase and LC3B-II is ligated to the forming autophagosome membrane. LC3B-II is found both on the outer and inner membrane of the forming autophagosome and is therefore degraded when autophagosome and lysosome fuse. This conversion and turnover of LC3B-I to LC3B-II is an indicator of autophagy induction and flux, however this process is cell specific and requires establishment of a LC3 turnover/conversion for each cell type used (Campbell et al., 2015; Campbell & Spector, 2013; Klionsky et al., 2016). A simplified version of the autophagy process can be viewed in figure 10.

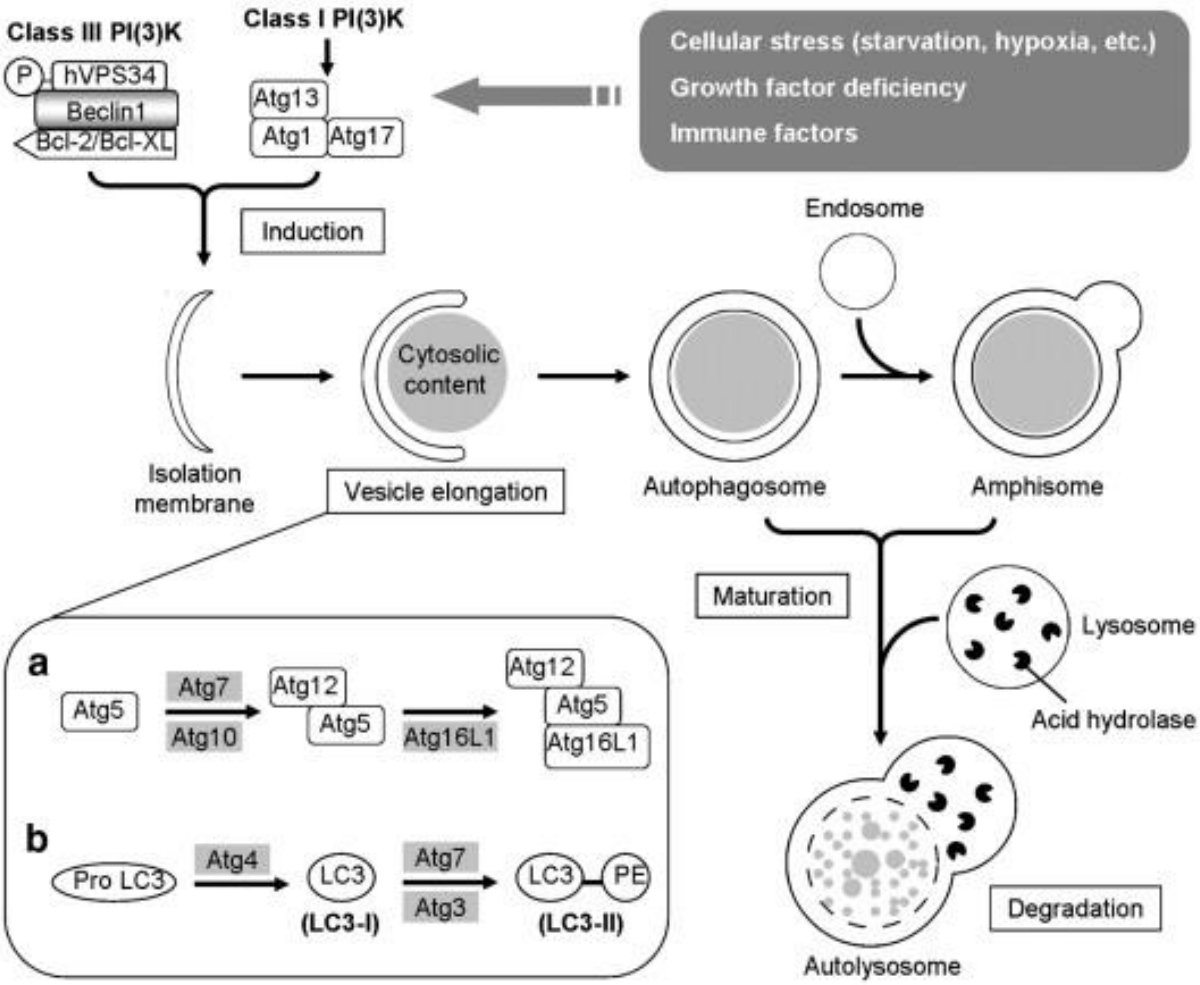

Figure 10 The autophagy process. Unfavorable cellular conditions activate the class I PI(3)K with Atg1 complex and class III PI(3)K complex including Beclin-1, they in turn activate downstream ATG proteins in several steps that control the induction, elongation, maturation, and degradation of the autophagosome. Vesicle elongation is directed by two ubiquitin-like conjugation systems, Atg12 (a) and LC3 (b). The membrane of the vesicle elongate forming a crescent shape around the cytoplasmic cargo. When the membrane is complete the autophagosome is remodeled as it matures by fusion with endosomes/lysosomes into an autolysosome and the autophagic vacuole along with its content is degraded. Reprinted from Virology, 402, (Lin et al., 2010), Viral interactions with macroautophagy: A double-edged sword., 10 Copyright (2010), with permission from Elsevier.

2 Aims

Overall aims of the project were to investigate the role of MVV Vif and examine alternative functions to APOBEC3 degradation during infection.

Specific aims were:

1. To examine the connection of Cyclophilin A and Vif. To determine the effects of Cyclophilin A binding on virus replication and APOBEC3 activity.
2. To examine possible effects of autophagy modulation by MVV in infected cells.
3. To determine if Vif has a role in autophagy modulation.

3 Materials and methods

3.1 Molecular clones

The infectious molecular clone KV1772 was used as a WT model in this study. KV1772 is a plaque-purified biological clone derived from KV1514. It was selected by neurovirolence in a serial passage of Icelandic sheep (Andresson et al., 1993). Duplication of the KV1772 LTR, containing the sequence CAAAT allows this virus strain to grow well in cells of neural origin, such as SCP cells (Agnarsdottir et al., 2000; Oskarsson et al., 2007). The proviral DNA of KV1772 is stored as two subclones on plasmids p8XSp5-RK1 and p67f (pBluescript II SK, from Stratagene). p8XSp5-RK1 contains the beginning of the virus genome starting with a sheep flanking sequence containing a StuI restriction site, continuing through the 5'LTR of the virus to an XbaI restriction site at position 7768. P67f on the other hand is the 3' molecular clone starting from the XbaI site at position 7768 to the end of the LTR. (Skraban et al., 1999). P8, a pUC19 vector containing a BamHI4587 -> HincII6392 fragment of the large p8XSp5-RK1 plasmid was used for construction of the P -> A 192 single mutant. Plasmid containing P->A mutations at sites 21 and 24 dubbed 3-4 (p8XSp5-RK1 backbone) was used for the construction of the triple mutant P21/24/192A. A list of plasmids used in this study can also be viewed in the appendix.

3.1.1 Primers

List of primers used in this project can be found in the appendix. All primers were previously designed by other members of the lab.

3.1.2 Construction of P192A and P21/24/192A, site directed mutagenesis

Insertion of a point mutation causing proline to alanine substitution at site 192 in Vif was performed using in vitro site directed mutagenesis. The method utilizes the Phusion® Hot start high-fidelity (HF) DNA polymerase with 3´ -> 5´ exonuclease activity. Two primers containing the desired mutation, VifP192AMspforw and VifP192AMsprev, as well as two non-mutagenic, 4620 and -5880, primers were used in a PCR reaction, temperature cycling can be seen in table 1.

The bands generated in the reaction were run and then extracted from a 1% agarose gel. Both bands were used as templates in a new PCR reaction, using the non-mutagenic primers producing a 1260bp band containing the desired mutation. Product was run on a gel and extracted.

The 1260bp band and an original p8XSp5-RK1 plasmid were digested with MluI and BglII at 37°C, run on a gel and extracted. The extraction products were ligated with T4 ligase at 15°C overnight and were now ready for transformation in E. coli. Reaction mixtures for digestion and ligation can be found in tables 2 and 3.

Table 1 Temperature cycling, site directed mutagenesis

Temperature [°C]	Time [min]	
94	5:00	
94	***0:30***	
55	***0:30***	***30 cycles***
72	***1:00***	
72	7:00	
4	∞	

Table 2 Restriction enzyme digestion mixture, site directed mutagenesis

DNA	100ng/reaction
NEBuffer 3	2µl
BglII	1µl
MluI	1µl
ddH2O	Total volume to 20µl

Table 3 Ligation mixture, site directed mutagenesis

	µl
p8XSp5-RK1 12ng/reaction	4
Mutated DNA 12ng/reaction	4
T4 buffer	1
T4 ligase 50 wiess U/µl	1

3.1.3 Construction of P192A and P21/24/192A, whole virus genome ligation

To join the p8XSp5-RK1 and p67f plasmids, 4,4µg of the larger plasmid, p8XSp5-RK1, and 1,6µg of the smaller p67f were used. Plasmids were digested with XbaII for 4h. XbaII was inactivated by heating to 65°C for 20 min and a 2µl sample was taken to check the restriction efficiency on an agarose gel. The two plasmids were ligated with T4 ligase overnight. The T4 ligase was inactivated by heating to 65°C for 15 min. A 2µl sample of the ligation was also taken to check ligation efficiency. Digestion and ligation mixtures can be viewed in table 4.

Table 4 Whole virus genome digestion/ligation mix

Digestion	µl
Large plasmid:	
P192A 154,74ng/µl	29
P21/24/192A 171,27ng/µl	26
P67f 500ng/µl	3,2
XbaII 10U/µl	2
Tango buffer x10	3,8
H_2O	Total volume 38µl
Ligation	
T4 ligase 50 wiess U/µl	1
T4 buffer DNA	4,5
H_2O	3,5

3.2 DNA and RNA methods

3.2.1 cDNA preparation

Supernatant from viral samples (see 3.4.4) was centrifuged at 14000rpm for 1 hour at 4°C. Supernatant was discarded and the virus pellet resuspended in 10µl of TNE. 9µl of viral solution and 2µl of 20µM primer -1818 were mixed together and allowed to anneal for 5 min at 65°C then cooled down to room temperature for 10 minutes. Using the High capacity cDNA reverse transcription kit from Applied Biosystems a master mix (table 5) was made and added to the sample, then the reaction was run on a temperature cycler. Master mix contents can be viewed in table 5 and the temperature cycling program in table 6.

Table 5 Master mix, cDNA

	µl
10x RT Buffer	2
dNTP 20mM	0,8
Multiscribe™ Reverse transcriptase	0,5
Rnase inhibitor	0,25
ddH2O	5,45

Table 6 Temperature cycling, cDNA

	Temperature [°C]	Time [min]
First reaction	65	5:00
	22	10:00
Second reaction	37	60:00
	90	5:00
	4	∞

3.2.2 DNA quantification

Concentration of DNA samples was measured using NanoDrop® ND-1000 spectrophotometer from NanoDrop Technologies Inc.

3.2.3 PCR

Polymerase chain reaction was performed using either Phusion (the Phusion® Hot start high-fidelity DNA polymerase from Thermo Scientific) or Taq polymerase (DreamTaq™ DNA polymerase from Thermo Scientific). Master mixes and temperature cycling can be seen in tables 7 and 8.

Table 7 PCR Master mixes

	Phusion polymerase reaction [µl]	Taq polymerase reaction [µl]
Template DNA	1-5	1-10
Buffer	10	2
dNTP [2 mM]	5	2
Primer forw [20µM]	2,5	1
Primer rev [20µM]	2,5	1
Polymerase 2U/µl or 5U/µl	1	0,5
ddH2O	Total volume to 50µl	Total volume to 20µl

Table 8 PCR temperature cycling

	Phusion/Taq polymerase reaction		
	Temperature [°C]	Time [min]	
Initial denaturation	98/95	5:00	
Denaturation	***98/95***	***0:30***	
Annealing	***55***	***0:30***	***15-30 cycles***
Extension	***72***	***1:00***	
Final extension	72	7:00	
	4	∞	

3.2.4 Agarose gel electrophoresis of DNA

Bacterial plasmids or PCR products were run on 1% agarose gels. Gels were made by melting agarose (Agarose basic by AppliChem) in TBE, cooled down to about 50°C, 1-3 drops of ethidium bromide (1µg/ml) added and allowed to solidify. Before loading, electrophoresis samples were mixed with 10x loading buffer. An appropriate ladder depending on the size of sample products was also used. The electrophoresis was run at 70-85V for 40 minutes to an hour depending on the size of the gel.

3.2.5 Gel extraction

DNA extraction was performed using the PCR clean up and gel extraction kit from Macherey-Nagel.

Gel was dissolved in NTI buffer (200µl per 100mg gel) and heated at 50°C for 5-10 min until completely dissolved. The solution was loaded on a NucleoSpin® gel and PCR Clean-up column with a collection tube and then centrifuged at 11000g for 30 sec, the DNA is now bound on the silica in the column. Column was washed twice with 700µl of NT3 buffer by centrifugation at 11000g for 30 sec, always discarding flow-through. The silica was dried by centrifuging once more at 11000g for 1 min. DNA was eluted by adding 15-30µl NE buffer and waiting for 1 min at room temperature before centrifuging at 11000g for 1 min. The flow-through was collected in a new micro centrifuge tube now containing the DNA and was stored at -20°C if not being used immediately.

3.2.6 Transformation of E. coli

Transformation was performed in DH5α chemically competent E. coli.

Bacterial cells were stored at -80°C and thawed on ice. 1-2 µl ligation or plasmid mix was added to the cells and stored on ice for 10 min. Cells were then heat shocked at 42°C for 1 min and placed back on ice for 2 min. 200µl of LB medium with 20mM glucose was added to the cells and they were incubated on a shaker for 1 hour at 37°C. Cells were now spread on LB agar with 100µg/ml ampicillin and incubated overnight at 37°C.

3.2.7 Isolation of DNA, bacterial plasmid

Plasmid DNA purification was performed using the Plasmid DNA purification kit from Macherey-Nagel.

Bacterial cells were harvested by pelleting cells in a centrifuge at 11000g for 30 sec. Supernatant was discarded and cells were resuspended in 250µl of buffer A1. 250µl of buffer A2 were then added and the solution mixed by inverting 6-8 times, then 300µl of buffer A3 was added and mixed by inverting. The cells were now completely lysed. The lysate was centrifuged at 11000g for 5-10 min and supernatant collected. The supernatant was loaded on a NucleoSpin® plasmid column and centrifuged at 11000g for 1 min. Flow-through was discarded and the DNA was now bound on the silica in the column. The column was washed twice with 600µl of A4 buffer by centrifugation at 11000g for 30 sec, always discarding flow-through. The silica was dried by centrifuging once more at 11000g for 2 min. DNA was eluted by adding 30-50µl AE buffer and waiting for 1 min at room temperature before centrifuging at 11000g for 1 min. The flow-through was collected in a new microcentrifuge tube now containing the DNA and stored at -20°C if not being used immediately.

3.2.8 Real time PCR

Analysis of infectivity was performed using RT-qPCR. Virus samples (3.4.4) were used to make cDNA (3.2.1) that was used for the infection analysis. 5µl of the cDNA is then used with 15µl of TaqMan qPCR master mix (Invitrogen). Samples were loaded in triplicates and compared to a 10^6 -10^3 copies of MVV KV1772 vector dilution. Master mix and temperature cycling can be viewed in tables 9 and 10.

Table 9 RT-qPCR Master mix

	µl
TaqMan Buffer	10
-1719 Primer 20µM	0,9
1636 Primer 20µM	0,9
Probe 1665 10µM	0,5
H_2O	2,7

Table 10 RT-qPCR temperature cycling

	Temperature [°C]	Time [min]	
Step 1	50	2:00	
Step 2	***95***	***0:10***	***40 cycles***
Step 3	***95***	***0:15***	
Step 4	60	1:00	

3.2.9 DNA for sequencing

3.2.9.1 Isolation of DNA for sequencing

DNA was isolated from infected cells based on the protocol for DNA purification from cultured cells found in the Gentra® Puregene® Handbook 06/2011, used with the Gentra® Puregene® cell kit from Qiagen.

Cells grown in a monolayer were washed with PBS then trypsinized for 5-10 min at 37°C. After the cells had detached they were moved to 1,5 ml microcentrifuge tube and centrifuged at 3000g for 5 min. Supernatant was discarded and the pellet washed with PBS, centrifuged at 13000g for 5 sec to pellet cells again. The supernatant was removed and 300µl of lysis solution were added to cells, mixed by pipetting up and down. 100µl of Protein precipitation solution were added and sample was vortexed vigorously for 20 sec, then centrifuged for 1 min at 13000g and the supernatant collected in a new 1,5ml microcentifuge tube. 300µl isopropanol were added and the solution was mixed by inverting 50 times. The sample was centrifuged for 1 min at 13000g, now the DNA was visible as a small white pellet. The supernatant was discarded and the tube drained. The DNA pellet was washed with 70% ethanol and then centrifuged again for 1 min at 13000g. Ethanol was discarded and the tube allowed to air dry.100µl of DNA hydration solution were added and the sample vortexed 5 sec at medium speed and then incubated at 65°C for 1 hour to dissolve the DNA. The sample was then incubated overnight with gentle shaking.

3.2.9.2 Producing more DNA for sequencing

From DNA samples in 3.2.9.1 a PCR was performed using the Phusion polymerase (3.2.3). Samples could be sent for sequencing either after cloning PCR products into pCR4-TOPO cloning vector (Invitrogen) or as PCR products amplified from vector. Sequencing was performed by Beckman Coulter Genomics, United Kingdom.

3.2.10 Reverse Transcription Assay

Reverse transcription assay was performed according to protocol for the EnzChek® Reverse Transcription Assay kit from Invitrogen.

0,05 µl/sample of Poly(A) ribonucleotide template and oligo$(T)_{16}$ primer were mixed together and allowed to bind for 1h at room temperature. Template/primer solution was diluted 200-fold into polymerization buffer and then aliquoted 20µl per sample into new microfuge tubes. 5µl viral samples in TNE were added to the mixture. A negative control containing only TNE was also used. Reaction was incubated for 10-60 min at room temperature then stopped by adding 2µl of 200mM EDTA to each reaction. Picogreen was diluted 345-fold in 1xTE buffer. Samples and 173µl of picogreen solution were loaded on a 96-well plate and absorbance measured at 485nm/535nM. Absorbance from controls was subtracted and absorbance relative to KV1772 calculated.

3.3 Cell cultures

Cells used in this project were sheep choroid plexus cells (SCP), fetal ovine synovial (FOS), blood derived sheep macrophages and human embryonic kidney cells (HEK 293T).

3.3.1 SCP, FOS and HEK293T cells

Cells were cultivated in monolayers in Dulbecco's modified eagle medium (DMEM) supplemented with 2mM glutamine, 10% lamb serum (SCP and FOS) or 5% fetal bovine serum (HEK293T) also containing 100IU/ml of penicillin (Pen) and 100IU/ml Streptomycin (Strep). Cells were kept at 37°C in humidified atmosphere of 5% CO_2.

3.3.2 Macrophages

200ml of fresh blood was collected from a healthy sheep by a veterinarian at Keldur. 5 ml of heparin were added to the flask before the blood was collected to prevent coagulation. Blood was diluted 1:1 in sterile PBS with 100IU/ml Pen/Strep. 25ml of diluted blood was pipetted carefully on top of 15ml of Histopaque -1077 (Sigma-Aldrich) in a 50ml centrifuge tube then centrifuged for 30 min at 2100 rpm and 20°C. After centrifuging, a white layer of mono- and lymphocytes can be seen in the middle of the tube. This layer was pipetted into a new tube, the tube filled up to 40ml with PBS and centrifuged again, this time at 2000rpm for 15 min at 20°C. Supernatant was discarded and the cell pellet resuspended in 2ml of red blood cell lysis buffer and incubated at room temperature for 3 min. PBS up to 40 ml was added and cells were centrifuged at 1200rpm for 15 min at 20°C. Supernatant was discarded and cells resuspended in PBS centrifuged at 1000rpm for 15 min at 20°C. This step was repeated until the suspension looked completely clear after centrifuging. Cells were then counted and assigned appropriately. The cells were incubated in DMEM with 15% lamb serum, $5 \cdot 10^5$M 2-mercaptoethanol and 100IU/ml PEN/Strep. The cells were allowed to mature for one week before being infected.

3.4 Transfection and infection

3.4.1 Liposome mediated transfection

Transfection of SCP, FOS or HEK293T cells was performed using Lipofectamine LTX (Invitrogen). Cells were washed and DMEM with 1% lamb serum without antibiotics was added to the cells. 6µg of DNA in 500µl of DMEM and 15µl of Plus reagent was mixed in a microcentrifuge tube in another tube 500µl of DMEM and 30µl of Lipofectamine were mixed. Solutions were then mixed together and incubated at room temperature for 5 – 20 min. The solution can now be added carefully to cells. Cells were kept at 37°C in humidified air with 5% CO_2.

3.4.2 Creating a new mutant virus

As mentioned in 3.1, creating new virus mutants requires using molecular clones on two plasmids which can then be transfected into cells which will produce the new mutant virus. For the creation of P192A and P21/24/192A virus, ligated plasmids containing the whole virus genome was transfected into SCP cells using Lipofectamine LTX (Invitrogen). The method can be viewed in 3.4.1. The infection can be monitored under a light microscope.

3.4.3 Infecting cells with virus

When using previously frozen virus samples, cells were first washed with PBS and new growth medium added to them, then 1 MOI of virus was added to the medium. Cells were then incubated at 37°C on a roller for 2h. Medium was then taken off and new added. Cells were kept at 37°C in humidified air with 5% CO_2. Infection can be monitored under a light microscope.

3.4.4 Viral sample collection

During infection experiments 500µl of supernatant from cells (SCP, FOS or macrophages) was collected on specific days, 500µl of new medium was added to the cells. The supernatant was centrifuged at 3000g for 3 min to get rid of possible cell debris then 200µl of the supernatant were transferred into two new Eppendorf tubes. Samples were then frozen down at -80°C.

3.5 Protein methods

3.5.1 Western blotting

3.5.1.1 Sample collection, western blotting

Cells were washed once with PBS then an appropriate amount of RIPA buffer with 1:100 PIC was added to the cells. Cells were lysed for 30 min on a shaker at 4°C. The lysate was collected in a cold microcentrifuge tube and centrifuged at 12000rpm for 10 min at 4°C. Supernatant was collected in a new cold tube and 6x sample buffer added. Samples were boiled at 95°C for 5 min. Samples were kept on ice for use the same day (LC3 samples) but frozen at -20°C for longer storage.

3.5.1.2 SDS-PAGE and wet transfer

Protein samples were loaded on a 12% SDS-PAGE gel. The proteins were separated at standard 200V for 1h, LC3 protein samples were however run at 90V for 20 min and then 120V for 70 min. After the run, the gel was placed in transfer buffer for 5-30 min. Proteins were transferred to a polyvinylidene fluoride (PVDF) membrane with pore size 0,2µm. The PVDF membrane needs to be activated in methanol for 30 sec before use then placed in transfer buffer for 5-30 min. Transfer was run at standard 100V for 1h or 90V for 2h for LC3 proteins.

3.5.1.3 Immunoblotting

PVDF membrane was blocked in 5% milk/BSA for 30 min to 1h, then 1°antibody solution was added to the membrane and allowed to bind overnight. The membrane was washed 3 times with TBS-T and then 2° antibody solution was added and allowed to bind for 1h. Antibody solutions were 3% BSA/milk in TBS-T including relevant antibody. BSA was used for LC3 experiments otherwise milk was used. A list of antibodies used can be found in the appendix 7.3.

3.5.1.4 HPR

Membrane can be developed using Pierce™ ECL Western Blotting Substrate (ThermoFirsher scientific) according to protocol.

3.5.1.5 Odyssey

Using fluorescent dyes that are conjugated to 2° antibodies (DyLight) the membranes can be scanned directly with Odyssey infrared imaging system.

3.5.2 Co-immunoprecipitation (co-IP)

3.5.2.1 Plasmids

Plasmids used in this study can be viewed in appendix. The codon optimized plasmid for P-S mutant was originally made for this study. Mutation was inserted into a WT codon optimized Vif plasmid (Vif-Flag, pcDNA4) using the Phusion polymerase protocol (3.2.3) with plasmids VifoptiP-Sforw and VifoptiP-Srev. PCR product was then treated with 1µl of Dpn1 (10U/µl) for 1h at 37°C. Iµl of dpn1 treated mixture is mixed with first half of ligation mixture containing a polynucleotide kinase and incubated for 1h at 37°C. Then second half is containing a T4 ligase added and incubated for 1h AT 37°C (table 11). Plasmid is now ready for transformation, see 3.2.6.

Table 11 Dpn1 site directed mutagenesis, ligation mixture

	µl
First step:	
10x T4 ligase buffer	0,5
T4 polynucleotide kinase 10 U/µl	0,5
H_2O	3
Second step:	
T4 ligase 50 weiss U/µl	0,5
10x T4 ligase buffer	0,5
H_2O	4

3.5.2.2 Co-IP protocol

Based on the FLAG® immunoprecipitation kit (Sigma-Aldrich) protocol, cells were washed with PBS containing 1,7mM EDTA, then lysis buffer with 1:100 PIC was added. Cells were lysed at 4°C for 30 min during which Flag resin was washed 4 times with wash buffer. Cell debris was pelleted with a 8000 rpm 5 min spin at 4°C. 20µl input sample was saved and rest of the supernatant was loaded on to the Flag resin. Proteins were allowed to bind to beads overnight at 4°C on a roller. Resin was washed 3 times with 500µl of wash buffer, spin at 1600g for 30 sec, washes were kept for further examination. Elution was performed using 3X Flag peptide where 100µl of wash buffer containing 150ng/µl 3X Flag peptide were loaded onto resin and incubated for 30 min with gentle shaking at 4°C. The supernatant was taken off resin as it should now contain the desired proteins. All samples were boiled with 6x sample buffer at 95°C for 5 min. Samples were run on an SDS-PAGE gel and immunoblotted (see 3.5.1.2 and 3.5.1.3). Flag-LC3 was a kind gift from Anne Simonsen, Oslo University.

3.6 Microscopy

3.6.1 Confocal microscopy

Macrophages were cultured on microscope chamber slides and infected with different viral mutants. Cells would then be fixed at certain time points.

3.6.1.1 Sample fixing

Based on Immunofluorescence Protocol with Methanol Fixation (IF Methanol-fixed) from Cell signaling. Medium was taken off, cells were covered with ice cold 100% methanol and fixed at -20°C for 15 min. Methanol was discarded and cells rinsed 3 times with PBS for 5 min each.

3.6.1.2 Immunostaining

Cells were blocked for 1h in blocking buffer at room temperature. Blocking buffer was discarded and 1° antibody solution was added to specimen and incubated overnight. Cells were washed 3 times with PBS for 5 min each then fluorochrome-conjugated 2° antibody in antibody dilution buffer was added and incubated in dark for 1-2h. Cells were washed once with PBS, 1:5000 DAPI was added to cells and incubated for 5 min before a final wash. Cells were sealed with fluoroshield and a coverslip was clued on top. A list of antibodies used can be found in the appendix.

3.6.1.3 Confocal imaging

Samples were examined in Olympus FV1200 confocal microscope using appropriate settings depending on immunostaining efficacy and cell type. DAPI signal intensity was used as guide while focusing and photos were taken at random areas of cell cultures.

3.6.2 Green fluorescence microscopy

To monitor transfection of HEK293T cells in co-IP experiments a plasmid containing green fluorescence protein (eGFP), would be used. GFP has a major excitation peak at 490nm and emission peak at 509nm. Cells were viewed in a DM IL LED inverted microscope (Leica).

3.7 Computer work

RT-qPCR results were analyzed using Microsoft excel 2013. Error bars in replication experiments, 4.1.1 show standard deviation of data points. A Fisher exact test was performed to evaluate significance of G-A hypermutations and GAA/GGA mutations, a two-way ANOVA was also used to evaluate difference in trinucleotide context between virus mutants in 4.1.2, statistics performed using GraphPad Prism version 7.00 for Windows. Figure 15 in 4.1.2 is generated using Hypermut form sequence data (Rose & Korber, 2000). Western blot images were analyzed using Fiji (Schindelin et al., 2012) and charts created using GraphPad Prism. One-way ANOVA, with Tukey's multiple comparisons test was used to evaluate normalized means ± s.e.m. in immunoblots.

4 Results

4.1 Binding of CypA and Vif

In a previous study, Kane et al (2015) unexpectedly found that whereas the Vif proteins of primate lentiviruses require the non-canonical co-factor CBFβ for Vif-E3 ligase stabilization, a novel cofactor, CypA, was required for MVV Vif –E3 ligase stabilization and anti-APOBEC3 activity. Based on CypA's natural affinity for proline residues, P to A mutations were created to examine Vif-CypA binding. Co-IP showed that binding between CypA and Vif remained intact for all prolines except for residues P21/P24 together and P192 alone (Kane et al., 2015).

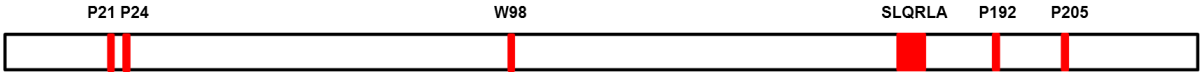

Figure 11 Amino acids of interest. P21, P24 and P192 show affinity for cyclophilin A binding. W98 is where Vif binds APOBEC3. P205 associated with the CA-Vif mutant has unknown function. W98R and P205S were used in Co-IP experiments. Mutating SLQ-AAA destroys Vif's binding to EloC of the ubiquitin ligase**.**

4.1.1 Effects of point mutations on virus replication

To determine the importance of Vif binding to CypA for viral replication, several virus mutants were constructed. Previously, mutants substituting alanine for proline at residues P21 and P24 as well as P21/P24 had been made. In the present study a virus mutant with a proline to alanine mutation at residue 192 and another with mutations at all three residual sites 21/24/192 were made. As a reference the WT virus KV1772 and SLQ-AAA were used. SLQ-AAA is unable to bind the ubiquitin ligase. Figure 11 shows the location of mutated amino acids in Vif used in this work. The nucleotide and amino acid sequences of KV1772 can be found in the appendix.

Replication was measured by RT-qPCR of cell-free supernatants of infected macrophage and SCP cell cultures, both natural targets of MVV infection. The results show that a WT virus (KV1772) replicated faster than all mutants as is to be expected. However comparing the mutants shows that single mutations on their own were not enough to severely debilitate the virus, but two (P21A/P24A) or three (P21A/P24A/P192A) mutations had a considerable effect on virus replication (figures 12-14). In SCP cells the triple mutant shows even lower rates than that of the double mutant (figure 14). Interestingly figure 14 also shows that the single mutant P192A has very low replication compared with the other single mutants P21A and P24A in Figure 12.

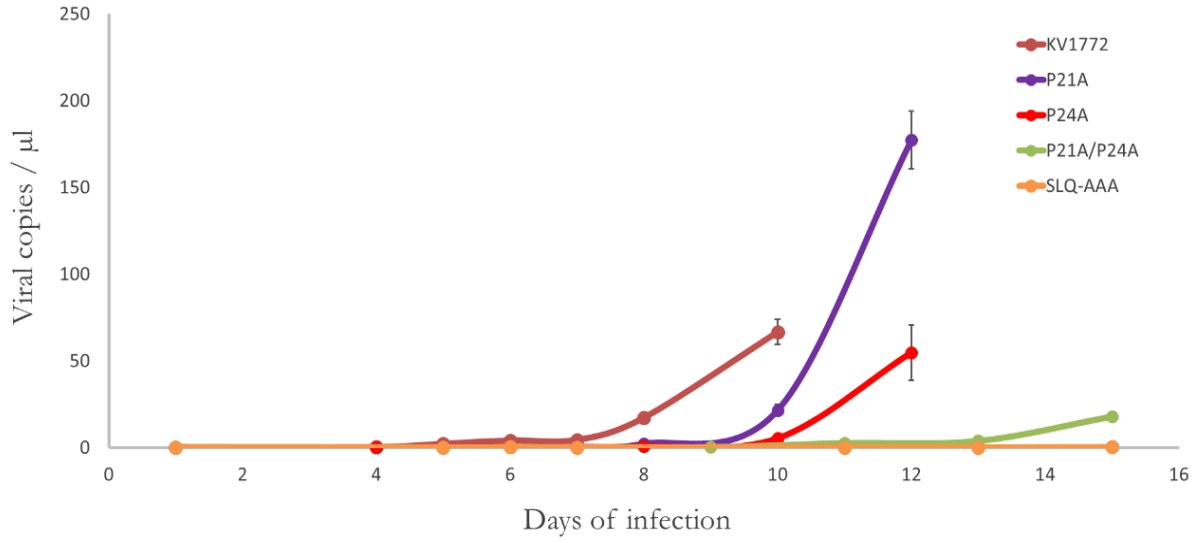

Figure 12 Viral replication in macrophages, mutants P21A, P24A and P21A/P24A. Infection experiment in macrophages. Viral production in the WT virus KV1772 starts on day 6 of infection. Viruses containing single mutations, P21A and P24A, show a slowed replication rate starting at days 9 and 10 respectively. A double mutant, P21A/P24A has considerably diminished production starting at day 13. SLQ-AAA shows almost no viral production. Error bars show S.D. of data points.

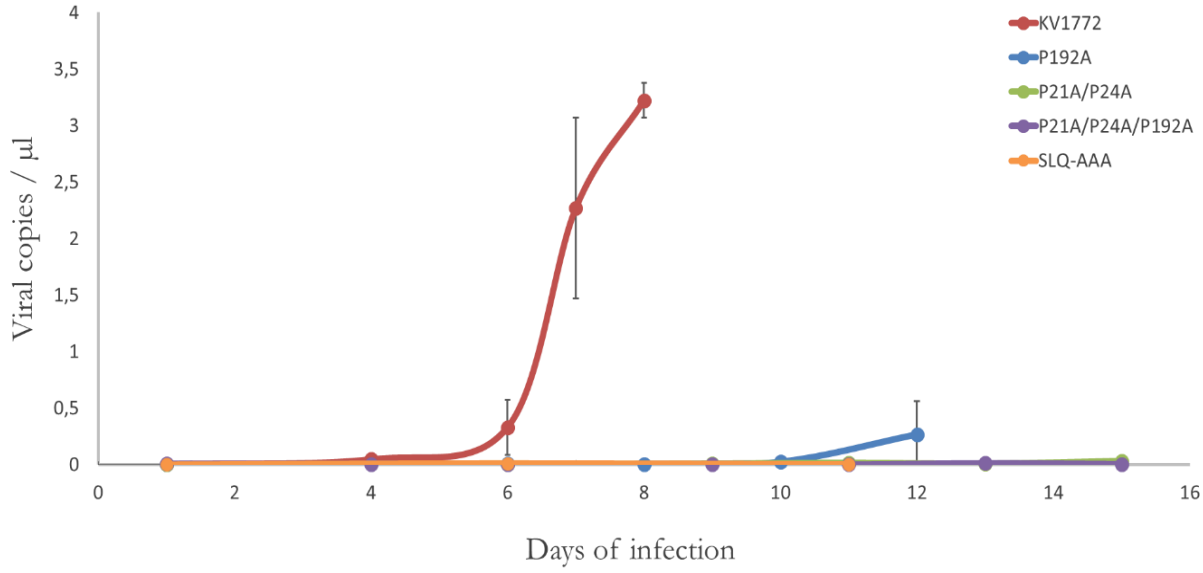

Figure 13 Viral replication in macrophages, mutants P192A, P21A/P24A and P21A/P24A/P192A. Infection experiment in macrophages. Viral production in the wt virus KV1772 starts on day 4 of infection. Viral mutants P192A shows slowed down production while P21A/P24A shows seriously diminished production as well as the triple mutant P21A/P24A/P192A, both replicating similar to SLQ-AAA. Error bars show S.D. of data points.

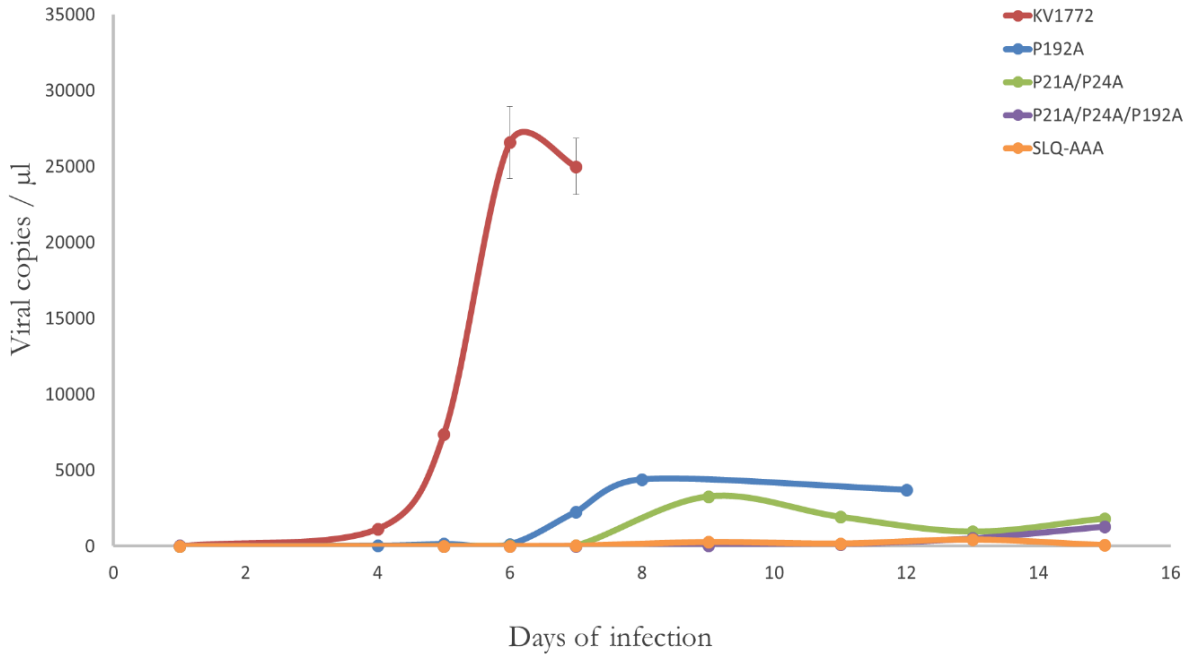

Figure 14 Viral replication in SCP cells, mutants P192A, P21A/P24A and P21A/P24A/P192A. Infection experiment in SCP cells. Viral production of KV1772 starts at day 4 of infection. The mutants all show a decreased rate of production with P21A/P24A/P192A falling in line with SLQ-AAA. Error bars show S.D. of data points.

4.1.2 G- A Hypermutations

To further examine the cause of diminished replication rates of the mutants P192A and P21A/P24A/P192A we sequenced DNA of incorporated viruses and looked for ABOPEC3 distinctive mutations. The APOBEC3 proteins of sheep recognize the trinucleotide context TTC and TCC for cytidine deamination resulting in G-A mutations in the trinucleotide context GAA and GGA on the plus-strand. A fragment of the *env* gene (nt 6911-7945) was amplified and cloned from proviral DNA.

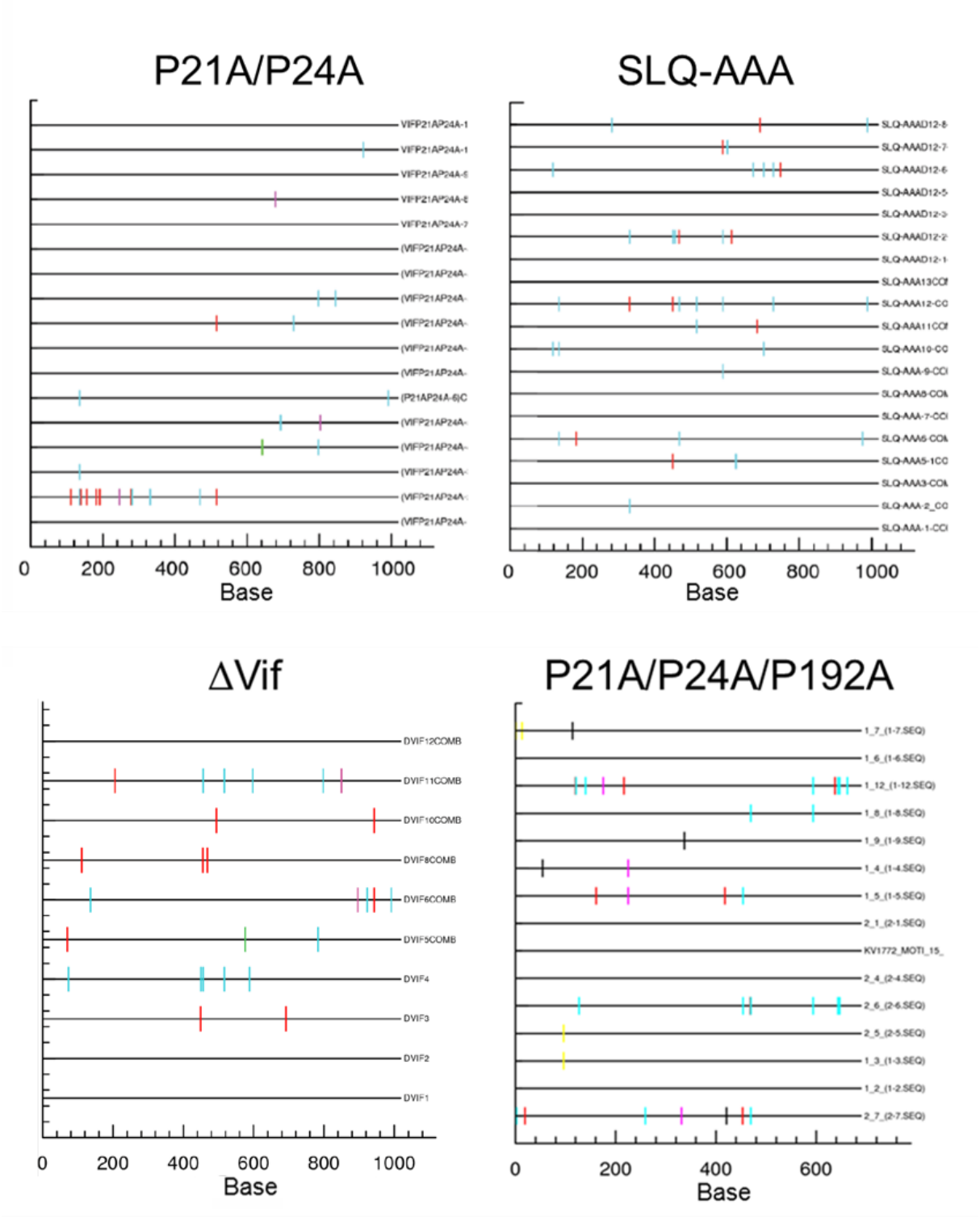

Figure 15 Nucleotide context of hypermutations. Shows the type of mutations found in each independent fragment where red = GG>AG, cyan = GA>AA green = GC>AC, magenta = GT>AT, black = not G>A transitions, yellow = gaps. Number of separate quantifications are as follows: P21A/P24A 17306 bp (n=17), SLQ-AAA 19342 (n=19), ΔVif 10890 bp (n=10) and P21A/P24A/P192A 10335 bp (n=15). Created using Hypermut (Rose & Korber, 2000).

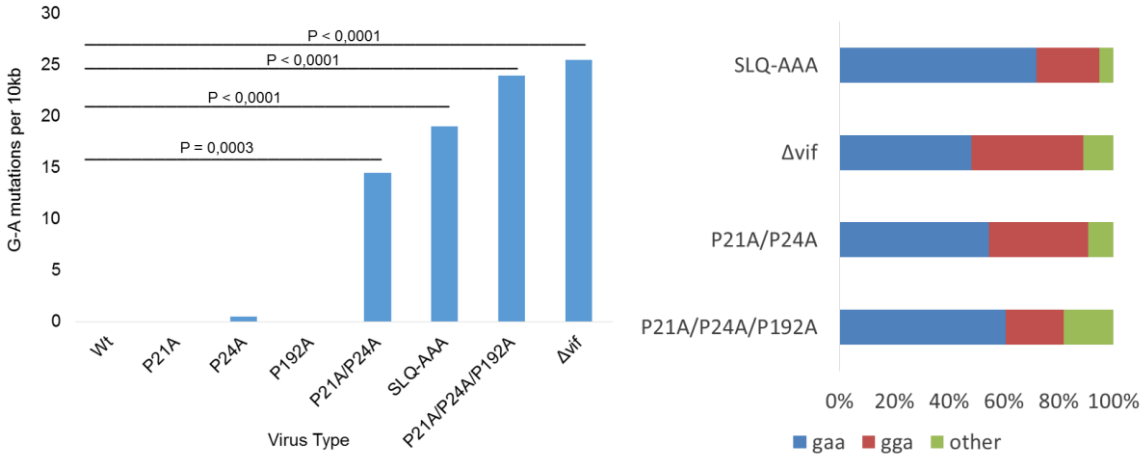

Figure 16 G-A hypermutation comparison between WT and mutant Vif types. To the left are numbers of G-A mutations per 10 kb of DNA. Single mutants show almost no APOBEC3 activity while the triple mutant P21A/P24A/P192A shows activity resembling a virus without the Vif protein (Δvif). Number of separate quantifications are as follows: WT 20360 bp (n=20), ΔVif 10890 bp (n=10), P21A 16288 bp (n=16), P24A 20360 bp (n=20), P192A 9636 bp (n=10), P21A/P24A 17306 (n=17), SLQ-AAA 19342 (n=19) and P21A/P24A/P192A 10335 bp (n=15). Significance calculated using Fisher's exact test. To the right is the trinucleotide context of G-A mutations with GGA and GAA being specific to sheep APOBEC3 activity. The double mutant shows context patterns similar to that of ΔVif. The triple mutant shows an increased rate for other mutations aside from the GAA/GGA context although more than 80% still qualify. Two-way ANOVA shows no statistical difference with mutation combination between virus types however a fisher exact test shows that the trinucleotide context GAA and GGA are highly significant compared with the rate of other G-A mutations, P<0,0001 for all mutants.

We found no mutations in the single mutant, P192A but several for the triple mutant where the majority of mutations were in the context of GAA and GGA. Results for SLQ-AAA, ΔVif and P21A/P24A were previously acquired by other members of the lab. Figure 15 shows the distribution and type of mutations found in each virus mutant generated using Hypermut (Rose & Korber, 2000). Analysis of the mutations in figure 16 shows that number of mutations are significant for SLQ-AAA, ΔVif, P21A/P24A and P21A/P24A/P192A, P=0,0003 for P21A/P24A and P<0,0001 for the other virus types. Figure 16 also shows that GAA/GGA mutations are not generated by chance (P<0,0001) and that between virus mutants there is little difference in mutation pattern.

4.2 MVV and autophagy in Macrophages

In order to determine if MVV modulates autophagy in sheep macrophages, we started by establishing working protocols for LC3 detection and co-immunoprecipitation. Protocols can be viewed in 3.5 and buffers found in the appendix.

To monitor infection and autophagic flux confocal imaging was used. The conversion of LC3-I which is found in the cytoplasm to LC3-II bound to the autophagosomal membrane, is a common readout for the induction of autophagy and autophagy flux. Immunofluorescent staining with an LC3 antibody followed by confocal imaging, allows the detection of LC3 puncta which are considered LC3-II positive autophagosomes. A more diffuse LC3 pattern is regarded cytoplasmic LC3-I (Klionsky et al., 2016). WT MVV is examined using confocal imaging as well as a ΔVif virus, a virus without the *vif* gene discussed in 1.1.1.2. To further test findings seen in confocal imaging, LC3 protein production was also examined using western blots. When lysates are run on a gel, LC3-II migrates faster than LC3-I, thus allowing the quantification of the two bands. We furthermore performed co-immunoprecipitation to test for a potential interaction of Vif and LC3 to start analyzing the mechanism by which autophagy is modulated.

Several virus types are examined in Co-IP experiments, SLQ-AAA, W98R and P205S. SLQ-AAA has AAA substituted for SLQ in the SLQRLA sequence making it incapable of ubiquitin ligase hijacking. W98R is unable to bind APOBEC3 and P205S (CA-Vif mutant, discussed in 1.1.1.2) has unknown function. Figure 11 shows the location of mutated amino acids in Vif used in this work. The nucleotide and amino acid sequences of KV1772 can be found in the appendix.

4.2.1 Confocal microspopy

Macrophages were infected with WT and ΔVif virus and fixed every day for the first days of infection. Antibodies for the viral capsid protein were used to monitor infection (Red) and LC3B (green) was used as an autophagy marker. DAPI (blue) was used to color the cell nuclei.

To examine the intensity of autophagic flux in macrophages, non-infected cells were treated with chloroquine. Chloroquine is an autophagy inhibitor, commonly known as a drug against malaria. Chloroquine works by raising the pH of lysosomes thereby blocking the enzymes that facilitated fusion of the lysosome and autophagosome (Shintani & Klionsky, 2004; Steinman et al., 1983). Treating macrophages with chloroquine shows a considerable increase in LC3 signal intensity, indicating the buildup of LC3 proteins inside the cells. Cells that are not treated with chloroquine show a moderate intensity indicating that autophagic flux is active.

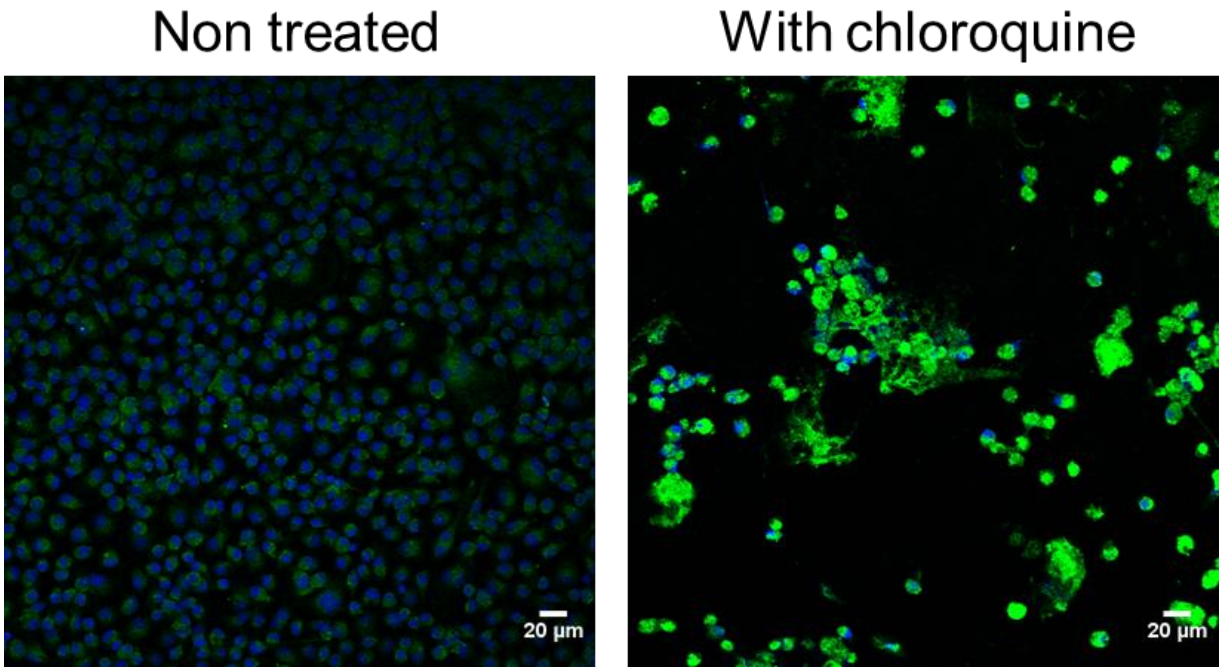

Figure 17 cloroquine treatment of non-infected macrophages. Macrophages that have been treated with the autophagy inhibitor chloroquine (right) show an increased signal intensity for LC3 proteins compared with non-treated controls (left). Scale bar represents 20µm.

Figure 18 shows the formation of a syncytium caused by the viral infection. After a few days of infection with a WT virus a syncytium starts to form, growing larger as the infection progresses. In a syncytium the nuclei form a three dimensional globe engulfed by cytoplasm, the middle usually shows a strong LC3 signal intensity indicating a high production (or buildup) of LC3 proteins and at the cell membrane viral capsid is distinct. The last surviving cells are mostly found in this type of syncytial giant cell before eventual death. Most cells in a WT infection will be lost during the first week of infection. The ΔVif mutant virus grows considerably slower with little adverse effects to the cell culture for the first two weeks as discussed in 1.1.1.2.

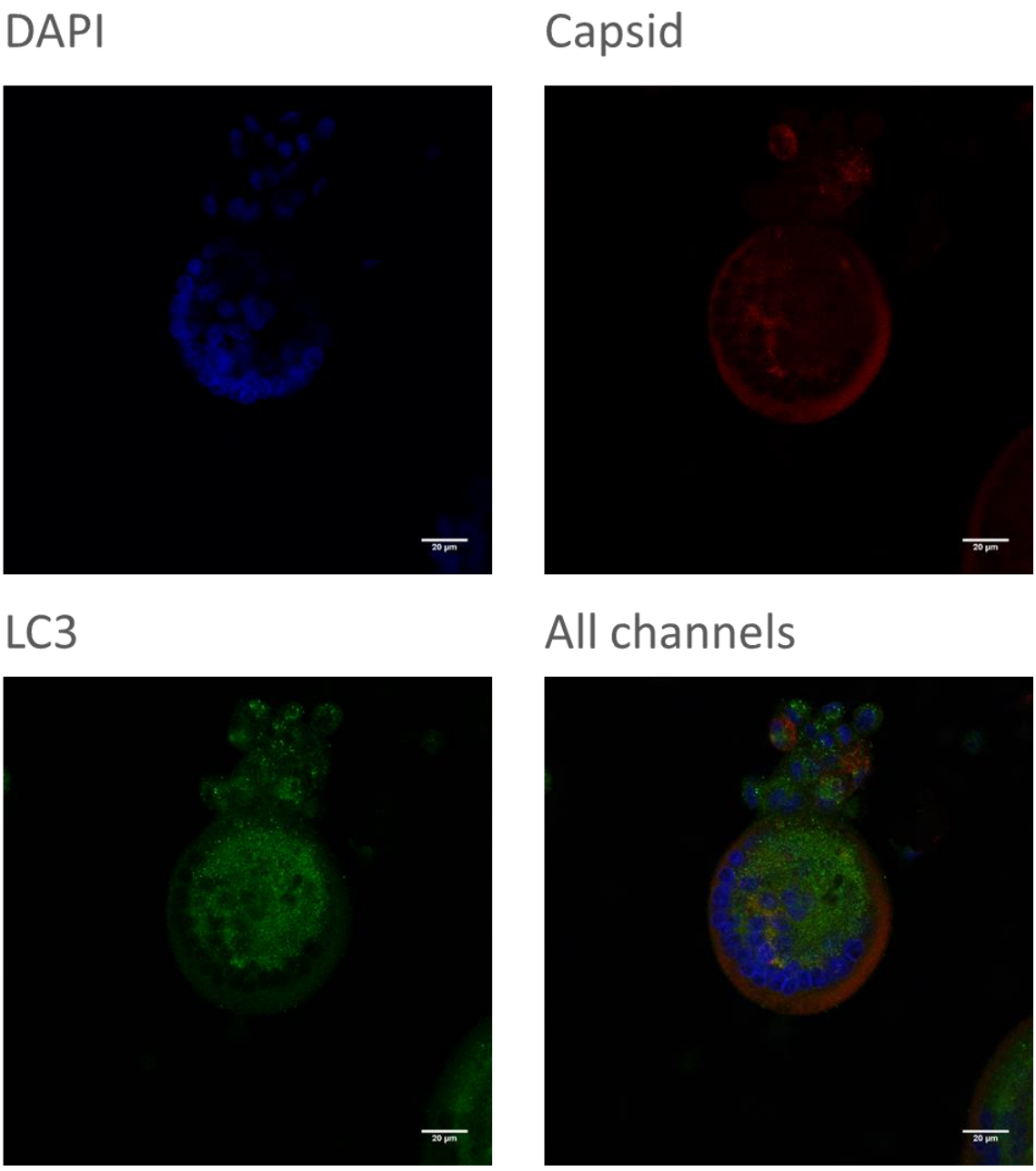

Figure 18 Syncytium at day 5 of a WT infection. Channels are shown separately for each dye DAPI, LC3 and capsid. Bottom right compilation of all channels, showing well the core of the syncytium with surrounding nuclei. The figure is representative for four independent experiments. Scale bar represents 20µm.

To monitor the autophagy response on different days following infection we stained for LC3 at days 1, 3 and 5 post infection (Figure 19). A noticeable reduction in LC3 intensity can be seen in a WT virus infection at day three of infection. Interestingly this effect is seen in all cells in the culture, not just what appear to be infected cells. To assay for a potential role of Vif in this autophagy response, we also stained for LC3 in macrophages infected with a ΔVif virus. Interestingly there is not a reduction in LC3 intensity on day 3 with the ΔVif virus.

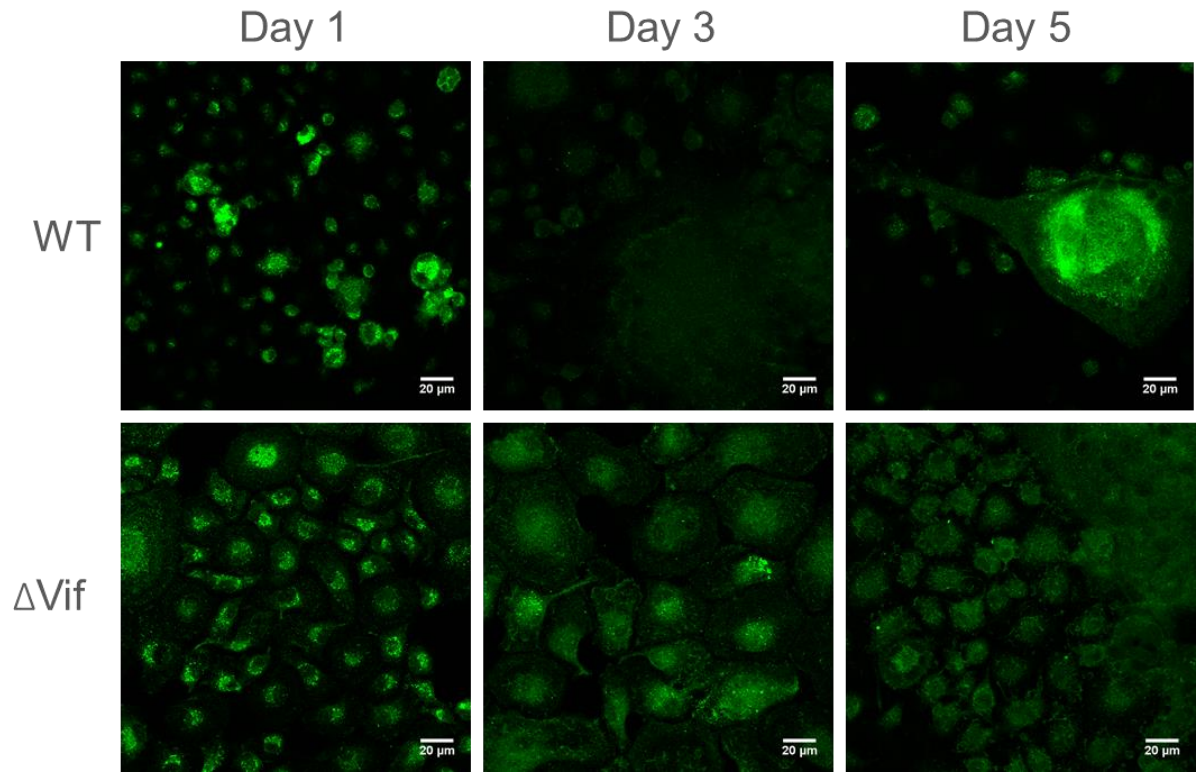

Figure 19 comparison of LC3 signal intensity between WT, Δvif and non-infected cells. Reduction in LC3 signal intensity can be seen in a WT infection at day 3. This reduction cannot be seen in a virus lacking the Vif protein. The figure is representative for four independent experiments. Scale bar represents 20µm.

We found interesting this difference in the autophagy response between WT and ΔVif on day 3 post infection. First, we tested for differences in LC3 intensity between infected and non-infected cells within the same WT culture at this time point, by co-staining for LC3 and Capsid (Figure 20). This showed that the LC3 staining was even in the culture regardless of whether cells were infected or not.

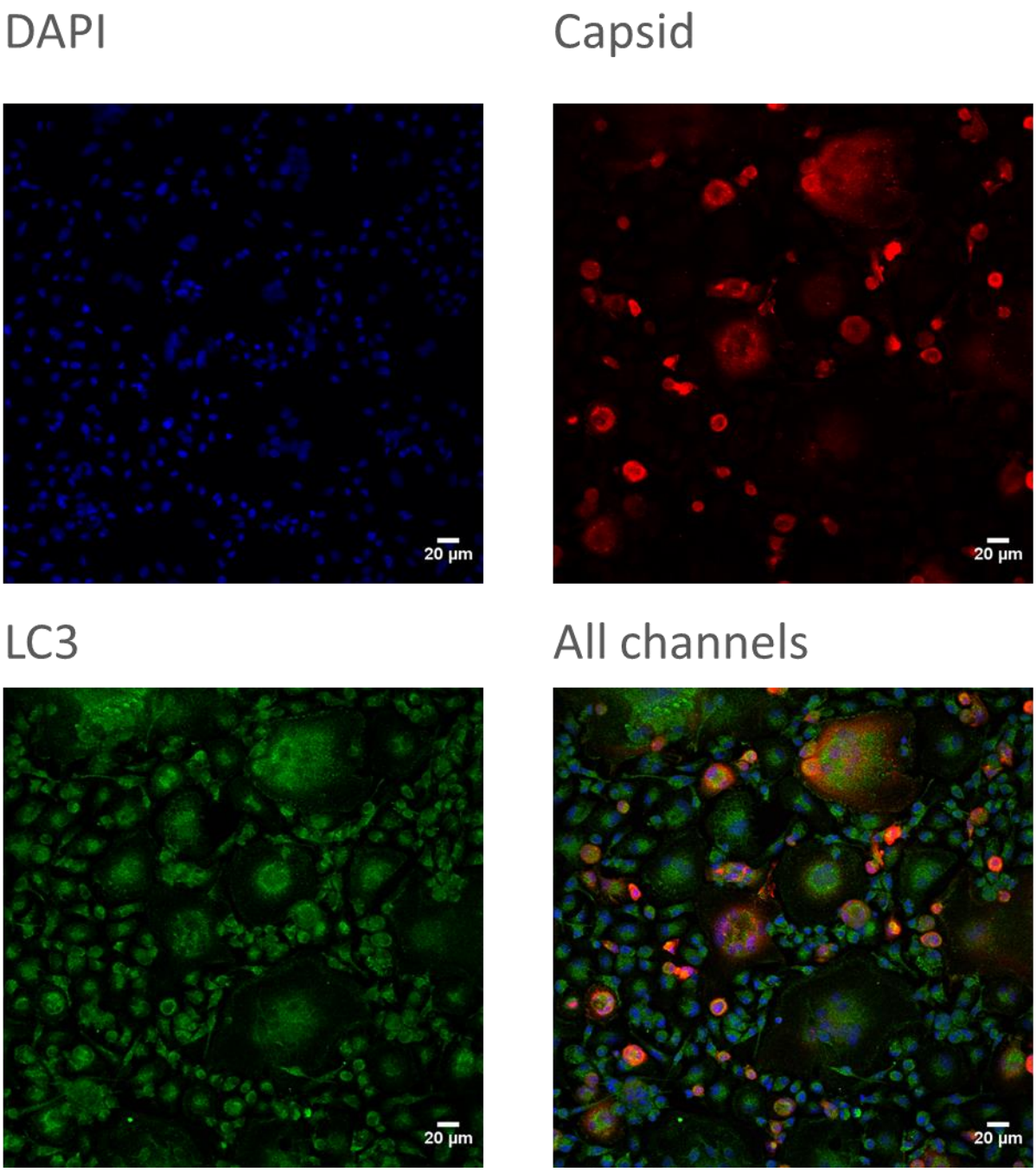

Figure 20 WT infection Day 3, all channels. The reduction in LC3 signal intensity can be seen in the whole cell culture not only infected cells. Scale bar represents 20µm.

Next we compared WT and ΔVif infected cells at this same time point (day 3 post infection). Again, we observed that WT infected macrophages had decreased LC3 staining in all cells in the culture (Figure 21). Interestingly, this was not the case for ΔVif infected macrophages as infected cell had increased LC3 staining compared with non-infected cells within the same culture (figure 20).

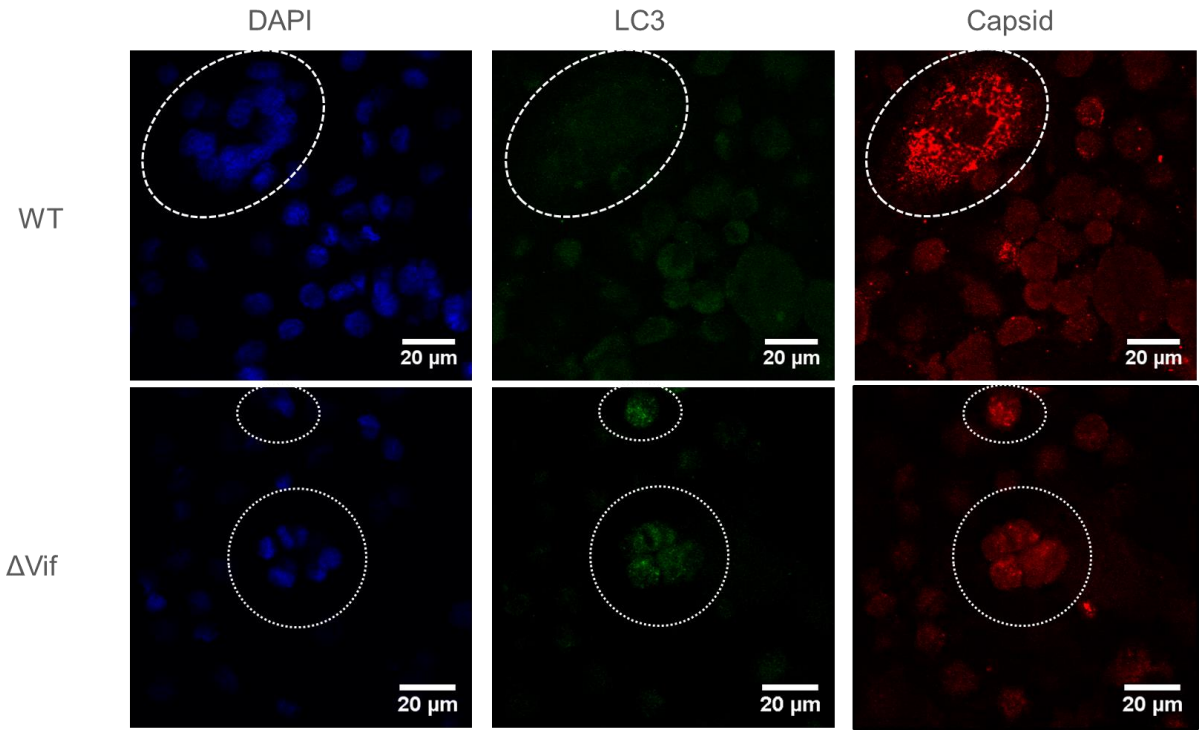

Figure 21 Comparing autophagy of infected cells at day 3 of WT and ΔVif infections. Same area is shown for all channels DAPI, LC3 and capsid. Noticeably in the area marked with a white dashed line no LC3 signaling is seen in a WT infection. In the ΔVif example virus infected cells show an increased LC3 signal. The figure is representative for four independent experiments. Scale bar represents 20µm.

4.2.2 Western blot results

To further analyze this difference in the autophagy response we also assayed for the LC3 marker using immunoblotting. Macrophages were infected with WT virus for several days, proteins were extracted and run immediately. We found it important for the detection of this small protein (14-16 kDa) to run the lysates without freezing them first. Blots were stained with LC3 and actin antibodies, using actin for normalizing for loading differences. A list of antibodies used in this work can be seen in the appendix.

Western blots showed an induction in LC3 production at day 2 post infection compared with non-infected cells (figure 22). A general reduction was also observed in overall LC3 production at days 3 and 4 of WT infection (figure 22). This is in agreement with the previous data from confocal analysis (figure 19).

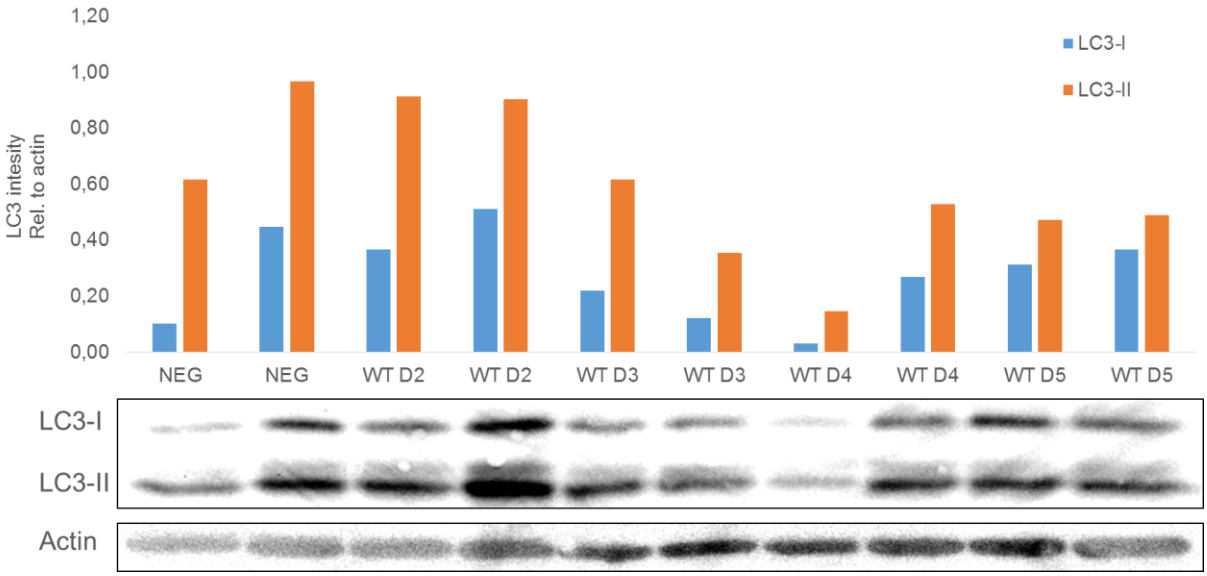

Figure 22 Representative western blot of WT virus infected macrophages. Shows β-actin and LC3 bands from a WT infection of macrophages on a western blot as well as a densitometric analysis done in imageJ of the same blot. A reduction of LC3 proteins is seen at days three and four. Samples with the same name are biological replicates.

Results from statistical analysis and estimation of significance in LC3 reduction can be seen in figure 23. Data from four separate experiments show a significant reduction in LC3-I protein reduction between days 2 – 3 and 2- 4 as well as a significant reduction in LC3-II between days 2 – 4.

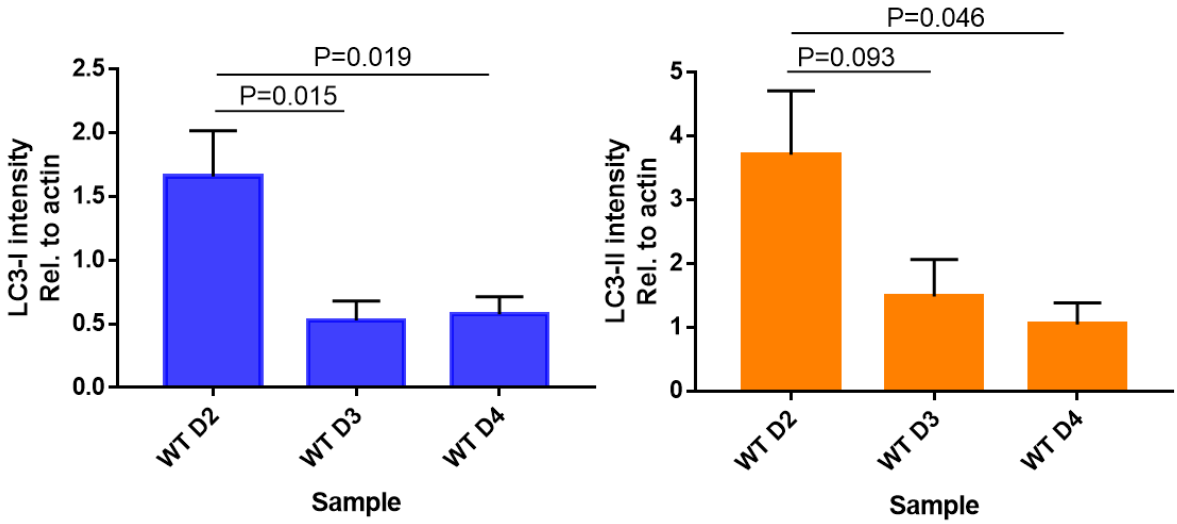

Figure 23 Comparison of LC3 I and II protein production days 2-4 of WT infection. Densitometric analysis of WT infection days 2-4 presented as means ± s.e.m., n = 4. One-way ANOVA shows significant decrease in LC3-I protein production from day 2 compared to both days 3 and 4. LC3-II protein production also shows a significant decrease in protein production from day 2 to 4. LC3-II production decrease from day 2 to day 3 is however not significant, P=0,093.

As primary monocytes take a week to develop into macrophages to be infected and the number of cells is limited we looked for a more efficient way to monitor LC3 protein production in virus infection. Figure 24 shows LC3 proteins from WT virus infected SCP cells. In macrophages LC3-II is usually in higher yields than LC3-I (figure 22). This is reversed in SCP cells showing a basic difference in general autophagy between the two cell types. The pattern of LC3-I vs. LC3-II observed in the SCP cells, is similar to what has been observed in other cells of neuronal origin (Klionsky et al., 2016). This experiment was only performed once and thus preliminary data and statistical analysis not possible. It is however interesting that the trend in LC3 reduction of WT at day 3 is also observed in these cells (figure 24).

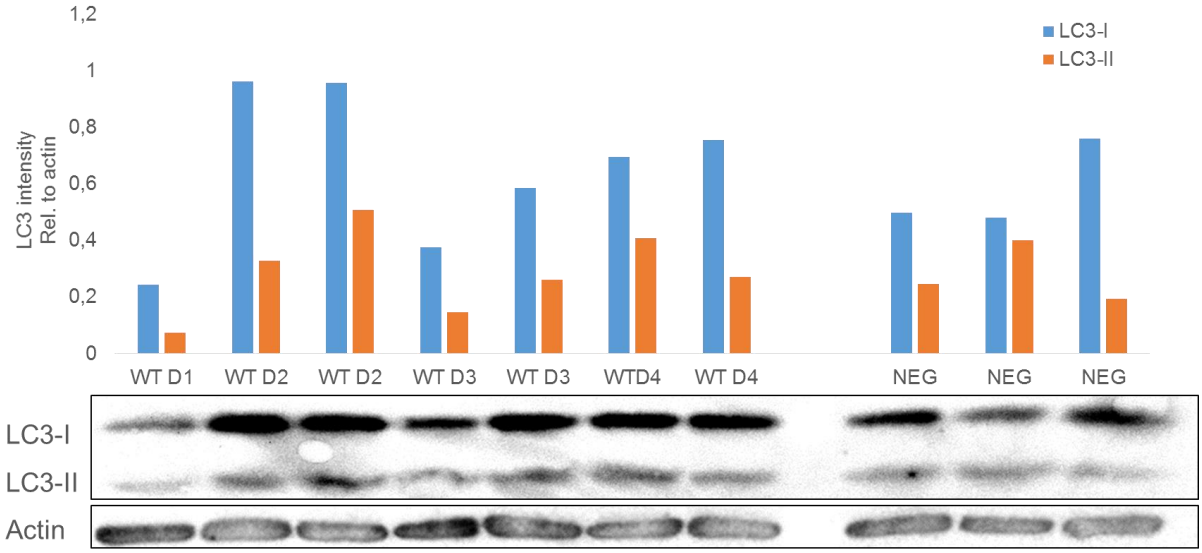

Figure 24 LC3 Western blot of WT virus infected SCP cells. Shows β-actin and LC3 bands from a WT infection of SCP cells on a western blot as well as a densitometric analysis done in imageJ of the same blot. SCP cells show a higher production of LC3-I than LC3-II. A reduction of LC3 proteins is also observed at day three of infection. Samples with the same name are biological replicates.

4.2.3 Co-IP results

Next we wanted to test if the difference of autophagy response between WT and ΔVif virus infected cells is due to direct interaction of Vif and LC3. First we used a Flag tagged Vif for pull down but did not obtain adequate results. Therefore LC3-Flag was used instead with previously made HA-tagged Vif proteins. LC3-Flag was pulled down by Flag antibody covered resin and WT Vif-HA as well as three Vif mutants P205S, W98R and SLQ-AAA were examined. We chose these mutants based on interesting phenotypes they exhibit in macrophages. SLQ-AAA is unable to bind the ubiquitin ligase, W98R is unable to bind APOBEC3 and P205S has unknown function (see CA-Vif in1.1.1.2) (figure 11).

Figure 25 shows the presence of tagged proteins in the cell lysate (input). After the washing steps proteins not bound to the resin are washed away. This can be seen by diminished amounts of protein after the third wash in figure 25. Samples are eluted with a competing 3x-flag peptide prior to running them on Western blot gels. We stained the blots with HA and Flag antibodies and observed that WT Vif

binds LC3. The mutant Vif (P205, W98R, SLQ-AAA) viruses that we tested also bind LC3. This implies that these amino acids are not important for the binding of Vif to LC3.

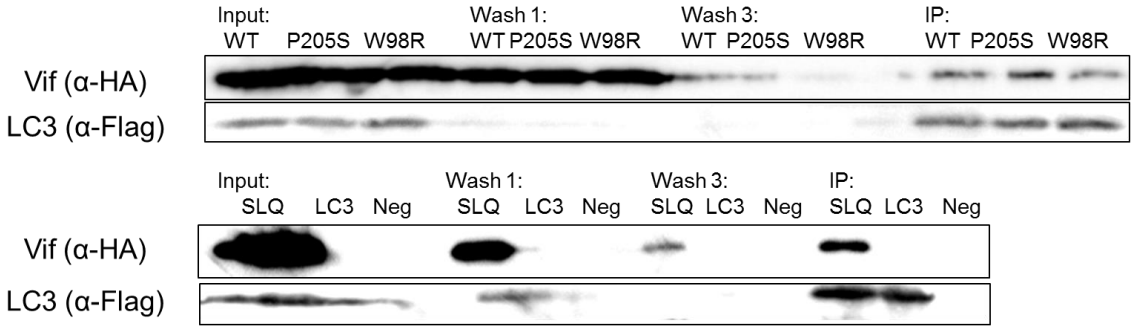

Figure 25 Co-IP results. HA-tagged Vif proteins are eluted with Flag-tagged LC3 proteins showing that they bind in the cell. Proteins checked for binding are WT Vif, Vif P205S, Vif W98R and Vif SLQ-AAA. Samples marked LC3 includes only LC3-Flag and Neg contains neither LC3-Flag nor a Vif protein.

5 Discussion

It is becoming increasingly clear that cellular restriction factors play an important role in the defense against microbial invasions. Throughout evolution several factors have evolved to protect against retroviral infections, for instance the APOBEC3 proteins, TRIM5α SAMHID1 and tetherin. As discussed in this work there is strong evidence that even more restriction factors are still unknown. Unfortunately retroviruses are highly capable of protecting themselves against host cell defenses due to high replication rates, slow progressing latent infections and high mutation rate. They have developed several specialized means of counter measures, such as the Vif proteins.

A key characteristic of viruses is their small size, due to their size and particularly small genome they cannot afford to carry extra genetic information that is not directly relevant to their continued existence, as Richard Dawkins describes in his book *the selfish gene* they are very capable survival machines. Because of size restrictions it would be highly beneficial for the viral proteins to have more than just a single function in the fight for survival. Further exploiting different reading frames and frameshifts the minimal genome can be used to its maximum capacity. Already many viral proteins have been shown to serve multiple functions e.g. the VP40 protein of Ebola virus (Bornholdt et al., 2013) and closer to home, Vpr of HIV-1. Vpr has multiple functions in HIV infection for example it facilitates nuclear localization of PIC, induces cell cycle arrest at G2/M phase, can activate transcription of viral proteins and induce apoptosis linked to the development of AIDS (Pandey et al., 2009).

The aims of this study were in part to examine the newly discovered CypA binding to MVV Vif as well as to examine alternative roles for MVV Vif, focusing on autophagy.

5.1 Binding of CypA and Vif

In order to see what effects Vif-CypA binding has on replication, the P192A and P21A/P24A/P192A mutants were constructed. They were used together with previously constructed mutants P21A, P24A and P21A/P24A. The results showed a clear relationship between the ability of Vif to bind CypA and virus replication. Single mutants P21A, P24A an P192A showed reduced replication rates, the double mutant containing P21A/P24A replicated even slower and the triple mutant P21A/P24A/P192A showing the slowest replication rates. To find out if CypA binding was necessary for Vifs ability to degrade APOBEC3, incorporated proviral DNA from cell culture was sequenced. The sequencing results showed that the triple mutant had a level of G-A hypermutation similar to that of a virus without Vif, indicating that it had lost the ability to degrade APOBEC3.

Although MVV capsid does not incorporate CypA into virus particles as the HIV capsid does, it is intriguing how these two related viruses can use the same protein for totally different functions. CypA is very abundant in the cytoplasm and therefore a convenient choice for virus hijacking. This is an example of how capable viruses are to adapt to their hosts.

To determine where these proline residues are binding to CypA it would be interesting to repeat this experiment using Cyclosporin, an inhibitor of CypA, which binds to its catalytic site. Hypothesizing that

P21 and P24 bind to the catalytic site and P192 binds elsewhere. Replication experiment with the single mutants would then show P192 replicating slower than the other two and with associated hypermutations, as Cyclosporin would compromise binding of the still functioning prolines, P21 and P24.

Proline residues are known to be structurally important for correct protein folding, this is a worry when creating point mutations that will remove possible cornerstones in the architecture of the protein. Kane et al. showed that the two proline residues P21 and P24 together were not enough to structurally compromise the Vif protein by co-affinity purifications, they showed that both P21A/P24A and SLQ-AAA were still able to properly bind OaA3Z2-Z3. This implies that the mutations prevent correct assembly of the CRL complex but not binding to substrates. Interestingly P192A alone seems to be enough to seriously debilitate virus production as seen in figures 13-14, however APOBEC3 activity is not seen with this mutant indicating that Vif is still structurally sound. P192A might be connected to another function of Vif that is still unknown.

5.2 MVV modulates autophagy in Macrophages

To determine if MVV infection has an effect on the autophagy process in primary sheep macrophages several experiments were carried out. The results showed that a MVV does indeed modulate autophagy by significantly restricting the production of LC3 proteins at days 3 and 4 of infection. Autophagy is then increased again and is especially apparent in the syncytium cells found later in the infection.

MVV was previously known to cause syncytium formation and syncytia are a common side effect of certain virus infections such as HIV, respiratory syncytial virus (RSV), paramyxoviruses and others (Delpeut et al., 2012; Lin et al., 2010; Owczarczyk et al., 2015). Viral fusion proteins expressed on the surface of infected cells can bind to a neighbor's receptor, merging the two together. The binding of receptors on their own can be enough to kick start autophagy induction as seen in the case of the CD46. The CD46 receptor found in humans is able to bind various pathogens where interaction alone is enough to activate a Beclin1/VPS34 mediated autophagy response (Joubert et al., 2009). This type of fusion mediated autophagy might explain some part of the response seen here both in the beginning of the infection and later as syncytia begins to from, as seen on the confocal images (figure 18).

The observation that LC3 levels were reduced in both infected and non-infected macrophages of a WT infected culture points towards a mechanism involving secretory factors. Our hypothesis regarding this effect is that infected cell must secrete regulatory factors that can through some process, or on their own, control transcription of LC3 proteins. It would be interesting to assay for the localization of factors important for LC3 transcription at the different time points. This could be done by co-staining for the transcription factor TFEB and monitor the localization at different time points. TFEB shuttles between the cytoplasm and nucleus depending on environmental stress factors that signal the need for transcription of autophagy related genes (Settembre et al., 2012). This shuttling response could be altered by the virus.

5.3 Vif is important for autophagy modulation in macrophages

Immunofluorescence analysis indicates a specific role for Vif in the modulation of the autophagy response following MVV infection. We observed by confocal imaging that unlike the WT virus, ΔVif infected macrophages did not have decreased LC3 levels at day 3 post infection. This will have to be assayed by Western blotting as well. We found that MVV Vif binds LC3, and while this work was in progress HIV Vif was shown to bind LC3 as well (Borel et al., 2015). As discussed in 1.3.1.3 the Vif protein has been hard to capture with crystallography, possibly Vif is highly malleable with different structural capabilities, able to bind many substrates with different functions. It is quite common for proteins to have different functions based on their structure, the fact that Vifs crystal structure has only been captured in complexes with other proteins gives some merit to this hypothesis. As shown in Kane et al., 2015, MVV Vif shows affinity for binding both Cullin 2 and 5 of the CRL ubiquitin ligase, in other words two separate CRL ligase complexes. It is unknown if Vif uses both of them in the degradation of APOBEC3. Theoretically if Vif uses them for separate degradation processes it is possible that the degradation of LC3 could be one of them. This might be a possibility as an overall reduction in LC3-I and LC3-II protein levels is seen in both confocal and western blot results as if they have been purposefully removed from the cytoplasm.

The Vif mutants used in Co-IP experiments were in part chosen to find out if their phenotype could be explained be autophagy modulation. The MVV mutant CA-Vif that has two single point mutations, one in the capsid and one in Vif P205S encounters some form of inhibition in both macrophages and FOS cells but not SCP cells. As the reasons for this are still unknown we tested to see if Vif with P205S was still able to bind LC3. Co-IP results show that P205S Vif can still bind LC3 and the phenotype associated with this virus still remains a mystery. The other mutants examined by Co-IP, W98R and SLQ-AAA were expected to bind LC3 as their phenotype has already been established although it would have been interesting if they were also unable to bind LC3 as that would have added a new dimension. Work to establish which domains of Vif are required for the LC3 binding is already in process in the laboratory.

The fact that SCP cells show a different LC3 pattern than that of macrophages is not surprising as cells of neuronal origin typically show higher yields of LC3-I due to their overall high basal autophagic flux (Cai et al., 2010). To continue this work it would be interesting to establish if overall loss of LC3 protein can also be seen in SCP cells.

The question of whether MVV is inducing autophagic flux or not is not answered in this work. Our results with changed levels of LC3 show changes in autophagy but monitoring LC3 proteins is on their own not an efficient way to establish whether or not autophagic flux is taking place. The specific patterns of LC3 proteins expression is cell type dependent and demands establishing a baseline pattern for each cell type used, using several different stressors/inhibitors (Klionsky et al., 2016). This can be done by starving the cells of nutrients and/or inhibiting the autophagosomal breakdown with inhibitors such as Chloroquine and BafilomycinA1. To establish if genuine induction of autophagic flux occurs in the first days of infection other factors have to be monitored. Factors such as SQSTM1, also known as p62, where inhibition of autophagy causes increase in SQSTM1 protein levels but during autophagic flux SQSTM1 is degraded in the autolysosomes and therefore shows reduced levels (Bjorkoy et al., 2009;

Campbell & Spector, 2013). It will also be important to monitor the changes in the autophagy flux by comparing the degradation of long lived proteins (LLPD) in WT and ΔVif infected cultures. By using autophagy specific inhibitors this allows direct monitoring of the autophagy flux.

We have established that during a MVV infection of macrophages autophagy modulation takes place that is dependent on MVV Vif. We showed that MVV Vif is able to bind LC3 proteins implicating that this binding may be a mechanism by which Vif modulates autophagy. It will be exciting to establish further how autophagy is modulated by Vif and dissect out the mechanism of this modulation.

6 Conclusion

The results show a clear relationship between point mutations of residues P21, P24 and P192 to alanine. Single mutations individually affected replication of the virus somewhat without G-A hypermutation, but the double mutant, P21A/P24A and triple mutant, P21A/P24AP192A replicated considerably slower than a wild type virus with significant increase in G-A mutations, with that triple mutant Vif P21A/P24A/P192A being even more attenuated and showing about the same amount of APOBEC3 activity as a MVV mutant without the Vif protein. This indicates that Cyclophilin A has a role in degrading APOBEC3 and is necessary for the correct function of MVV Vif.

This work shows that MVV modulates autophagy during infection of primary sheep macrophages. Macrophages infected with MVV show a temporary change in autophagy on third and fourth day of infection and LC3 protein levels are diminished during this time. This change is in part Vif mediated as a virus without *Vif* does not show the same effect. In addition, MVV Vif protein binds to the LC3 protein, a key player in the autophagy system. These findings indicate a new and previously unknown function of MVV Vif.

References

Acheampong, E., Rosario-Otero, M., Dornburg, R., & Pomerantz, R. J. (2003). Replication of lentiviruses. *Front Biosci, 8*, s156-174.

Agnarsdottir, G., Thorsteinsdottir, H., Oskarsson, T., Matthiasdottir, S., Haflidadottir, B. S., Andresson, O. S., & Andresdottir, V. (2000). The long terminal repeat is a determinant of cell tropism of maedi-visna virus. *J Gen Virol, 81*(Pt 8), 1901-1905.

Akari, H., Fujita, M., Kao, S., Khan, M. A., Shehu-Xhilaga, M., Adachi, A., & Strebel, K. (2004). High level expression of human immunodeficiency virus type-1 Vif inhibits viral infectivity by modulating proteolytic processing of the Gag precursor at the p2/nucleocapsid processing site. *J Biol Chem, 279*(13), 12355-12362.

Allen, P., Collins, B., Brown, D., Hostomsky, Z., & Gold, L. (1996). A specific RNA structural motif mediates high affinity binding by the HIV-1 nucleocapsid protein (NCp7). *Virology, 225*(2), 306-315.

Andresson, O. S., Elser, J. E., Tobin, G. J., Greenwood, J. D., Gonda, M. A., Georgsson, G., Andresdottir, V., Benediktsdottir, E., Carlsdottir, H. M., & Mantyla, E. O. (1993). Nucleotide sequence and biological properties of a pathogenic proviral molecular clone of neurovirulent visna virus. *Virology, 193*(1), 89-105.

Bagashev, A., & Sawaya, B. E. (2013). Roles and functions of HIV-1 Tat protein in the CNS: an overview. *Virology Journal, 10*(1), 1-20.

Barre-Sinoussi, F., Ross, A. L., & Delfraissy, J.-F. (2013). Past, present and future: 30 years of HIV research. *Nat Rev Micro, 11*(12), 877-883.

Bjorkoy, G., Lamark, T., Pankiv, S., Overvatn, A., Brech, A., & Johansen, T. (2009). Monitoring autophagic degradation of p62/SQSTM1. *Methods Enzymol, 452*, 181-197.

Borel, S., Robert-Hebmann, V., Alfaisal, J., Jain, A., Faure, M., Espert, L., Chaloin, L., Paillart, J. C., Johansen, T., & Biard-Piechaczyk, M. (2015). HIV-1 viral infectivity factor interacts with microtubule-associated protein light chain 3 and inhibits autophagy. *Aids, 29*(3), 275-286.

Bornholdt, Z. A., Noda, T., Abelson, D. M., Halfmann, P., Wood, M. R., Kawaoka, Y., & Saphire, E. O. (2013). Structural rearrangement of ebola virus VP40 begets multiple functions in the virus life cycle. *Cell, 154*(4), 763-774.

Cai, Q., Lu, L., Tian, J. H., Zhu, Y. B., Qiao, H., & Sheng, Z. H. (2010). Snapin-regulated late endosomal transport is critical for efficient autophagy-lysosomal function in neurons. *Neuron, 68*(1), 73-86.

Campbell, G. R., Rawat, P., Bruckman, R. S., & Spector, S. A. (2015). Human Immunodeficiency Virus Type 1 Nef Inhibits Autophagy through Transcription Factor EB Sequestration. *PLoS Pathog, 11*(6), e1005018.

Campbell, G. R., & Spector, S. A. (2013). Inhibition of Human Immunodeficiency Virus Type-1 through Autophagy. *Curr Opin Microbiol, 16*(3), 349-354.

Clements, J. E., & Zink, M. C. (1996). Molecular biology and pathogenesis of animal lentivirus infections. *Clin Microbiol Rev, 9*(1), 100-117.

Coffin, J. M., H., H. S., & E., V. H. (1997). *Retroviruses*: Cold Spring Harbor Laboratory Press.

De Guzman, R. N., Wu, Z. R., Stalling, C. C., Pappalardo, L., Borer, P. N., & Summers, M. F. (1998). Structure of the HIV-1 nucleocapsid protein bound to the SL3 psi-RNA recognition element. *Science, 279*(5349), 384-388.

Delpeut, S., Rudd, P. A., Labonté, P., & von Messling, V. (2012). Membrane Fusion-Mediated Autophagy Induction Enhances Morbillivirus Cell-to-Cell Spread. *J Virol, 86*(16), 8527-8535.

Dong, X., & Levine, B. (2013). Autophagy and viruses: adversaries or allies? *J Innate Immun, 5*(5), 480-493.

Espert, L., Denizot, M., Grimaldi, M., Robert-Hebmann, V., Gay, B., Varbanov, M., Codogno, P., & Biard-Piechaczyk, M. (2006). Autophagy is involved in T cell death after binding of HIV-1 envelope proteins to CXCR4. *J Clin Invest, 116*(8), 2161-2172.

Franzdottir, S. R., Olafsdottir, K., Jonsson, S. R., Strobel, H., Andresson, O. S., & Andresdottir, V. (2016). Two mutations in the vif gene of maedi-visna virus have different phenotypes, indicating more than one function of Vif. *Virology, 488*, 37-42.

Freed, E. O. (2001). HIV-1 replication. *Somat Cell Mol Genet, 26*(1-6), 13-33.

Fridriksdottir, V., Gunnarsson, E., Sigurdarson, S., & Gudmundsdottir, K. B. (2000). Paratuberculosis in Iceland: epidemiology and control measures, past and present. *Vet Microbiol, 77*(3-4), 263-267.

Glick, D., Barth, S., & Macleod, K. F. (2010). Autophagy: cellular and molecular mechanisms. *J Pathol, 221*(1), 3-12.

Gonda, M. A. (1994). Molecular biology and virus-host interactions of lentiviruses. *Ann N Y Acad Sci, 724*, 22-42.

Gudmundsson, B., Jonsson, S. R., Olafsson, O., Agnarsdottir, G., Matthiasdottir, S., Georgsson, G., Torsteinsdottir, S., Svansson, V., Kristbjornsdottir, H. B., Franzdottir, S. R., Andresson, O. S., & Andresdottir, V. (2005). Simultaneous mutations in CA and Vif of Maedi-Visna virus cause attenuated replication in macrophages and reduced infectivity in vivo. *J Virol, 79*(24), 15038-15042.

Gudnadottir, M., & Palsson, P. A. (1967). Transmission of maedi by inoculation of a virus grown in tissue culture from maedi-affected lungs. *J Infect Dis, 117*(1), 1-6.

Guo, Y., Dong, L., Qiu, X., Wang, Y., Zhang, B., Liu, H., Yu, Y., Zang, Y., Yang, M., & Huang, Z. (2014). Structural basis for hijacking CBF-beta and CUL5 E3 ligase complex by HIV-1 Vif. *Nature, 505*(7482), 229-233.

He, C., & Levine, B. (2010). The Beclin 1 interactome. *Curr Opin Cell Biol, 22*(2), 140-149.

Jonsson, S. R., Hache, G., Stenglein, M. D., Fahrenkrug, S. C., Andresdottir, V., & Harris, R. S. (2006). Evolutionarily conserved and non-conserved retrovirus restriction activities of artiodactyl APOBEC3F proteins. *Nucleic Acids Res, 34*(19), 5683-5694.

Joubert, P. E., Meiffren, G., Gregoire, I. P., Pontini, G., Richetta, C., Flacher, M., Azocar, O., Vidalain, P. O., Vidal, M., Lotteau, V., Codogno, P., Rabourdin-Combe, C., & Faure, M. (2009). Autophagy induction by the pathogen receptor CD46. *Cell Host Microbe, 6*(4), 354-366.

Kane, J. R., Stanley, D. J., Hultquist, J. F., Johnson, J. R., Mietrach, N., Binning, J. M., Jonsson, S. R., Barelier, S., Newton, B. W., Johnson, T. L., Franks-Skiba, K. E., Li, M., Brown, W. L., Gunnarsson, H. I., Adalbjornsdottir, A., Fraser, J. S., Harris, R. S., Andresdottir, V., Gross, J.

D., & Krogan, N. J. (2015). Lineage-Specific Viral Hijacking of Non-canonical E3 Ubiquitin Ligase Cofactors in the Evolution of Vif Anti-APOBEC3 Activity. *Cell Rep, 11*(8), 1236-1250.

Karn, J., & Stoltzfus, C. M. (2012). Transcriptional and Posttranscriptional Regulation of HIV-1 Gene Expression. *Cold Spring Harb Perspect Med, 2*(2).

Katz, R. A., & Skalka, A. M. (1994). The retroviral enzymes. *Annu Rev Biochem, 63*, 133-173.

Klionsky, D. J., Abdelmohsen, K., Abe, A., Abedin, M. J., Abeliovich, H., Acevedo Arozena, A., Adachi, H., Adams, C. M., Adams, P. D., Adeli, K., Adhihetty, P. J., Adler, S. G., Agam, G., Agarwal, R., Aghi, M. K., Agnello, M., Agostinis, P., Aguilar, P. V., Aguirre-Ghiso, J., Airoldi, E. M., et al. (2016). Guidelines for the use and interpretation of assays for monitoring autophagy (3rd edition). *Autophagy, 12*(1), 1-222.

Kristbjornsdottir, H. B., Andresdottir, V., Svansson, V., Torsteinsdottir, S., Matthiasdottir, S., & Andresson, O. S. (2004). The vif gene of maedi-visna virus is essential for infectivity in vivo and in vitro. *Virology, 318*(1), 350-359.

Kroemer, G., & Levine, B. (2008). Autophagic cell death: the story of a misnomer. *Nat Rev Mol Cell Biol, 9*(12), 1004-1010.

Kyei, G. B., Dinkins, C., Davis, A. S., Roberts, E., Singh, S. B., Dong, C., Wu, L., Kominami, E., Ueno, T., Yamamoto, A., Federico, M., Panganiban, A., Vergne, I., & Deretic, V. (2009). Autophagy pathway intersects with HIV-1 biosynthesis and regulates viral yields in macrophages. *J Cell Biol, 186*(2), 255-268.

LaRue, R. S., Andresdottir, V., Blanchard, Y., Conticello, S. G., Derse, D., Emerman, M., Greene, W. C., Jonsson, S. R., Landau, N. R., Lochelt, M., Malik, H. S., Malim, M. H., Munk, C., O'Brien, S. J., Pathak, V. K., Strebel, K., Wain-Hobson, S., Yu, X. F., Yuhki, N., & Harris, R. S. (2009). Guidelines for naming nonprimate APOBEC3 genes and proteins. *J Virol, 83*(2), 494-497.

LaRue, R. S., Lengyel, J., Jonsson, S. R., Andresdottir, V., & Harris, R. S. (2010). Lentiviral Vif degrades the APOBEC3Z3/APOBEC3H protein of its mammalian host and is capable of cross-species activity. *J Virol, 84*(16), 8193-8201.

Li, H., Dou, J., Ding, L., & Spearman, P. (2007). Myristoylation is required for human immunodeficiency virus type 1 Gag-Gag multimerization in mammalian cells. *J Virol, 81*(23), 12899-12910.

Lin, L. T., Dawson, P. W., & Richardson, C. D. (2010). Viral interactions with macroautophagy: a double-edged sword. *Virology, 402*(1), 1-10.

Lu, Z., Bergeron, J. R., Atkinson, R. A., Schaller, T., Veselkov, D. A., Oregioni, A., Yang, Y., Matthews, S. J., Malim, M. H., & Sanderson, M. R. (2013). Insight into the HIV-1 Vif SOCS-box-ElonginBC interaction. *Open Biol, 3*(11), 130100.

Lyall, J. W., Solanky, N., & Tiley, L. S. (2000). Restricted species tropism of maedi-visna virus strain EV-1 is not due to limited receptor distribution. *J Gen Virol, 81*(Pt 12), 2919-2927.

Malashkevich, V. N., Singh, M., & Kim, P. S. (2001). The trimer-of-hairpins motif in membrane fusion: Visna virus. *Proc Natl Acad Sci U S A, 98*(15), 8502-8506.

Malim, M. H., & Bieniasz, P. D. (2012). HIV Restriction Factors and Mechanisms of Evasion. *Cold Spring Harb Perspect Med, 2*(5), a006940.

Martina, J. A., Diab, H. I., Li, H., & Puertollano, R. (2014). Novel roles for the MiTF/TFE family of transcription factors in organelle biogenesis, nutrient sensing, and energy homeostasis. *Cell Mol Life Sci, 71*(13), 2483-2497.

Nigro, P., Pompilio, G., & Capogrossi, M. C. (2013). Cyclophilin A: a key player for human disease. *Cell Death Dis, 4*, e888.

Obchoei, S., Wongkhan, S., Wongkham, C., Li, M., Yao, Q., & Chen, C. (2009). Cyclophilin A: potential functions and therapeutic target for human cancer. *Med Sci Monit, 15*(11), Ra221-232.

Oskarsson, T., Hreggvidsdottir, H. S., Agnarsdottir, G., Matthiasdottir, S., Ogmundsdottir, M. H., Jonsson, S. R., Georgsson, G., Ingvarsson, S., Andresson, O. S., & Andresdottir, V. (2007). Duplicated sequence motif in the long terminal repeat of maedi-visna virus extends cell tropism and is associated with neurovirulence. *J Virol, 81*(8), 4052-4057.

Owczarczyk, A. B., Schaller, M. A., Reed, M., Rasky, A. J., Lombard, D. B., & Lukacs, N. W. (2015). Sirtuin 1 Regulates Dendritic Cell Activation and Autophagy during Respiratory Syncytial Virus-Induced Immune Responses. *J Immunol, 195*(4), 1637-1646.

Pandey, R. C., Datta, D., Mukerjee, R., Srinivasan, A., Mahalingam, S., & Sawaya, B. E. (2009). HIV-1 Vpr: a closer look at the multifunctional protein from the structural perspective. *Curr HIV Res, 7*(2), 114-128.

Petroski, M. D., & Deshaies, R. J. (2005). Function and regulation of cullin-RING ubiquitin ligases. *Nat Rev Mol Cell Biol, 6*(1), 9-20.

Rasaiyaah, J., Tan, C. P., Fletcher, A. J., Price, A. J., Blondeau, C., Hilditch, L., Jacques, D. A., Selwood, D. L., James, L. C., Noursadeghi, M., & Towers, G. J. (2013). HIV-1 evades innate immune recognition through specific cofactor recruitment. *Nature, 503*(7476), 402-405.

Rose, P. P., & Korber, B. T. (2000). Detecting hypermutations in viral sequences with an emphasis on G --> A hypermutation. *Bioinformatics, 16*(4), 400-401.

Sarafianos, S. G., Marchand, B., Das, K., Himmel, D. M., Parniak, M. A., Hughes, S. H., & Arnold, E. (2009). Structure and function of HIV-1 reverse transcriptase: molecular mechanisms of polymerization and inhibition. *J Mol Biol, 385*(3), 693-713.

Schindelin, J., Arganda-Carreras, I., Frise, E., Kaynig, V., Longair, M., Pietzsch, T., Preibisch, S., Rueden, C., Saalfeld, S., Schmid, B., Tinevez, J.-Y., White, D. J., Hartenstein, V., Eliceiri, K., Tomancak, P., & Cardona, A. (2012). Fiji: an open-source platform for biological-image analysis. *Nat Meth, 9*(7), 676-682.

Settembre, C., Di Malta, C., Polito, V. A., Garcia Arencibia, M., Vetrini, F., Erdin, S., Erdin, S. U., Huynh, T., Medina, D., Colella, P., Sardiello, M., Rubinsztein, D. C., & Ballabio, A. (2011). TFEB links autophagy to lysosomal biogenesis. *Science, 332*(6036), 1429-1433.

Settembre, C., Zoncu, R., Medina, D. L., Vetrini, F., Erdin, S., Erdin, S., Huynh, T., Ferron, M., Karsenty, G., Vellard, M. C., Facchinetti, V., Sabatini, D. M., & Ballabio, A. (2012). A lysosome-to-nucleus signalling mechanism senses and regulates the lysosome via mTOR and TFEB. *Embo j, 31*(5), 1095-1108.

Shintani, T., & Klionsky, D. J. (2004). Autophagy in Health and Disease: A Double-Edged Sword. *Science, 306*(5698), 990-995.

Shors, T. (2011). *Understanding viruses* (2nd ed.): Jones & Bartlett Learning.

Sigurdsson, B., Grimsson, H., & Palsson, P. A. (1952). Maedi, a chronic, progressive infection of sheep's lungs. *J Infect Dis, 90*(3), 233-241.

Sigurdsson, B., Palsson, P., & Grimsson, H. (1957). Visna, a demyelinating transmissible disease of sheep. *J Neuropathol Exp Neurol, 16*(3), 389-403.

Sir, D., & Ou, J. H. (2010). Autophagy in viral replication and pathogenesis. *Mol Cells, 29*(1), 1-7.

Skraban, R., Matthiasdottir, S., Torsteinsdottir, S., Agnarsdottir, G., Gudmundsson, B., Georgsson, G., Meloen, R. H., Andresson, O. S., Staskus, K. A., Thormar, H., & Andresdottir, V. (1999). Naturally occurring mutations within 39 amino acids in the envelope glycoprotein of maedi-visna virus alter the neutralization phenotype. *J Virol, 73*(10), 8064-8072.

Sonigo, P., Alizon, M., Staskus, K., Klatzmann, D., Cole, S., Danos, O., Retzel, E., Tiollais, P., Haase, A., & Wain-Hobson, S. (1985). Nucleotide sequence of the visna lentivirus: relationship to the AIDS virus. *Cell, 42*(1), 369-382.

Stanley, B. J., Ehrlich, E. S., Short, L., Yu, Y., Xiao, Z., Yu, X. F., & Xiong, Y. (2008). Structural insight into the human immunodeficiency virus Vif SOCS box and its role in human E3 ubiquitin ligase assembly. *J Virol, 82*(17), 8656-8663.

Steinman, R. M., Mellman, I. S., Muller, W. A., & Cohn, Z. A. (1983). Endocytosis and the recycling of plasma membrane. *J Cell Biol, 96*(1), 1-27.

Sundquist, W. I., & Kräusslich, H. G. (2012). HIV-1 Assembly, Budding, and Maturation. *Cold Spring Harb Perspect Med, 2*(7).

Thormar, H. (2005). Maedi-visna virus and its relationship to human immunodeficiency virus. *AIDS Rev, 7*(4), 233-245.

Thormar, H. (2013). The origin of lentivirus research: Maedi-visna virus. *Curr HIV Res, 11*(1), 2-9.

Thormar, H., & Cruickshank, J. G. (1965). THE STRUCTURE OF VISNA VIRUS STUDIED BY THE NEGATIVE STAINING TECHNIQUE. *Virology, 25*, 145-148.

Villet, S., Bouzar, B. A., Morin, T., Verdier, G., Legras, C., & Chebloune, Y. (2003). Maedi-visna virus and caprine arthritis encephalitis virus genomes encode a Vpr-like but no Tat protein. *J Virol, 77*(17), 9632-9638.

von Schwedler, U., Song, J., Aiken, C., & Trono, D. (1993). Vif is crucial for human immunodeficiency virus type 1 proviral DNA synthesis in infected cells. *J Virol, 67*(8), 4945-4955.

Ward, K. N., McCartney, A. C., & Thakker, B. (2009). *Notes on medical microbiology*: Churchill Livingstone

Weiss, R. A. (2006). The discovery of endogenous retroviruses. *Retrovirology, 3*(1), 1-11.

Wirawan, E., Lippens, S., Vanden Berghe, T., Romagnoli, A., Fimia, G. M., Piacentini, M., & Vandenabeele, P. (2012). Beclin1: a role in membrane dynamics and beyond. *Autophagy, 8*(1), 6-17.

7 Appendix

7.1 Vif sequences

KV1772 Vif nucleotide sequence

atgtta agttcatacc gccaccaaaa gaaatacaaa aagaataaag caagggagat aggaccccag ttgccactat gggcatggaa agaaacagca tttagtataa atcaggaacc ctattggtat agtaccataa ggctacaagg gttgatgtgg aataaaagag ggcataaact tatgtttgta aaagaaaacc aagggtatga gtattgggaa acatcaggaa aacagtggaa aatggagata agacgagatt tggatctgat agcccaaata aattttagaa atgcatggca atataaaagc cagggagaat ggaaaacaat aggggtctgg tatgaatcac caggggatta caagggaaaa gagaatcagt tttggttcca ttggagaata gctctctgca gctgtaacaa aacaaggtgg gatatacggg aattcatgat agggaagcat aggtgggatt tatgtaaatc gtgtatacaa ggggagatag ttaagaatac aaatccaaga agcttacaac gcttagcttt attgcaccta gcaaaagacc atgtatttca agtaatgcca ttgtggagag cccggagagt cacagtgcag aagtttccat ggtgtcgtag cccaatgggt tacacgatac cttggtctct gcaggaatgc tgggaaatgg aatccatctt tgaataa

KV1772 Vif amino acid sequence and mutations sites shown in red

1 M L S S Y R H Q K K Y K K N K A R E I G **P** Q L **P** L W A W K E T A F S I N Q E P Y W Y S T

45 I R L Q G L M W N K R G H K L M F V K E N Q G Y E Y W E T S G K Q W K M E I R R D L D

88 L I A Q I N F R N A **W** Q Y K S Q G E W K T I G V W Y E S P G D Y K G K E N Q F W F H W

131 R I A L C S C N K T R W D I R E F M I G K H R W D L C K S C I Q G E I V K N T N P R **SL Q**

175 **R L A** L L H L A K D H V F Q V M **P** L W R A R R V T V Q K F **P** W C R S P M G Y T I P W S

218 L Q E C W E M E S I F E

Vif codonoptimized with HA tag

Atgctctcca gttacaggca ccagaagaaa tataaaaaga acaaggcccg ggagataggc ccccagctgc cactgtgggc atggaaagaa acagcattct ctatcaatca ggagcccta ctggtatagc actattagact gcaggggctg atgtggaaca agcgaggcca taagctgatg tttgtgaagg aaaatcaggg ctacgaatat tgggaaacct cagggaagca gtggaagatg gaaatcagaa gggatctgg acctgatcgc tcagatcaatt ttcgcaacgc ttggcagtac aagtcccagg gggaatggaa gacaattggg gtgtggtacg agagccccgg agactacaag ggaaaagaga accaattctg gttccactgg cggattgccc tctgcagctg taacaagacc aggtgggaca tcagagagttt atgattgggaa gcacaggtggg acctgtgcaaa agctgcatcca gggcgagatt gtcaaaaaca ctaaccccag aagcctgcag agacttgccc tgcttcacct cgctaaggat catgtgttcc aggtcatgcc tctttggagg gcacggaggg tgactgtgca aaagttccca tggtgcaggt ctccaatggg atacaccatc ccctggagtc tgcaggagtg ttgggagatg gagagcattt ttgagtaccc atacgacgtc ccagattatg cgtag

7.2 Primers

Table 12 List of primers

Name	Sequence
VifP192Amsprev	5´-GTA TTT CAA GTA ATG GCA TTG TGG AGA GCC CGG AG-3´
VifP192Amsforw	5´-CTC CGG GCT CTCCAC AAT GCC ATT ACT TGA AAT AC-3´
V-4620EcoRI	5´-GTA GAG ACA CAT CAG ACG-3’
V-5880	5´-TTC TTC TAA CTG CAG CTC CC-3´
-1818Xbal	5´-GCT CTA GAT TAC AAC ATA GGC GGC GCG GA-3´
V-1719	5´-TCC CAC AAT GAT GGC ATA TTA TTC-3´
V1636	5´-TAA ATC AAA AGT GTT ATA ATT GTG GGA-3´
V1665 TaqMan	5´-Fam–CCA GGA CAT CTC GCA AGA CAG TGT AGA CA-BHQ-1-3
VifopotiP-Sforw	5´-GTG CAA AAG TTC TCA TGG TGC AGG-3´
VifoptiP-Srev	5´-CCT GCA CCA TGA GAA CCT TTG CAC-3´
V6911BamH1	5´-ATT CCA AAG GGA TCC GAA ATA ATA CC-3´
-7945bANh1	5´-CGC GGA TCC CAC AAT AAC CAA GCC CCC-3´

7.3 Antibodies

Table 13 List of antibodies

Name	type	Other info	Dilution
LC3B (2775S, Cell Signaling)	1° Rabbit		1:1000 western 1:200 cofocal
Monoclonal ANTI-FLAG® M2 (F3165, Sigma-Aldrich)	1°mouse		1:5000 western
Anti-Ha (Produced at keldur)	1° mouse		1:5000 western
Anti-Cyclophilin A antibody (ab41684, abcam)	1° rabbit		1:2000 western
Anti-Actin monoclonal (MAB1501, Millipore)	1° mouse		1:2000 western
Anti-P24 (Produced at Keldur)	1° mouse		1:5000 western 1:1000 confocal
Alexa Fluor 555 (A21428, Life Technologies Corporation)	2° Goat α-rabbit	Excitation max 555nm Emission max 565nm	1:1000 confocal
Alexa Fluor 546 (A11003, Invitrogen)	2° goat α-mouse	Excitation max 556 Emission max 573	1:1000 confocal
Alexa Fluor 488 (A11070, Life Technologies Corporation)	2° Goat α-rabbit	Excitation max 490nm Emission max 525nm	1:1000 confocal
Anti-mouse IgG H+L DyLight™ 800 4X PEG Conjugate (5257, Cell signaling)	2° mouse	Excitation max 777nm Emission max 794nm	1:15000 western
Anti-rabbit IgG (H+L) DyLight™ 680 Conjugate (5366, Cell signaling)	2° Rabbit	Excitation max 684nm Emission max 715nm	1:15000 western

7.4 Plasmids

Table 14 List of plasmids

Name	Parent plasmid	type
p8XSp5-RK1	pBluescript II SK	Molecular clone
P8	pUC19	Molecular clone
P67f	pBluescript II SK	Molecular clone
P192A	pBluescript II SK	Molecular clone
P3A	pBluescript II SK	Molecular clone
LC3-Flag	pDest	
LC3-GFP	pEGFP-LC3 (Addgene plasmid # 24920)	
Vif-Flag	pcDNA4	Codon optimized Vif
P205S-Flag	pcDNA4	Codon optimized Vif
Vif-HA	pVR1012	Codon optimized Vif
P205S-HA	pVR1012	Codon optimized Vif
W98R-HA	pVR1012	Codon optimized Vif
SLQ-HA	pVR1012	Codon optimized Vif
TOPO cloning vector	pCR4-TOPO	

7.5 Buffers and solutions

TNE buffer

0.1% Triton X-100, 10 mM Tris at pH 7.5, 100 mM NaCl and 1 mM EDTA at pH 7.5.

Red blood cell lysis buffer

0,14M NH_4Cl, 0,02M Tris, pH7,2

Mediums for culturing E. coli

LB medium

1% Tryptone, 0.1% Yeast extract, 1% NaCl

LB agar

1% Tryptone, 0.1% Yeast extract, 1% NaCl, 1.5% Bacto agar

Gel electrophoresis buffers

0.5x Tris borate-EDTA (TBE)

0.045 M Tris borate, 0.001 M EDTA

10X Restriction buffer (RSB)

50% glycerol, 15 mM EDTA, 0.25% bromophenol blue

Protein buffers

RIPA Buffer

20 mM Tris-HCl (pH 7,5), 150 mM NaCl, 1 mM Na2EDTA, 1 mM EGTA, 1% Np-40, 1% Sodium Deoxycholate

2x Sample buffer

0.5% 2-mercaptoethanol, 20% glycine, 2% SDS, 0.1%Bromophenol blue, 130 mM Tris

6x Sample buffer

40% Glycerol, 240 mM Tris (pH 6,8), 8% SDS, 0,04% Bromphenol Blue, 5% β-mercaptoethanol

Running Buffer

25 mM Tris, 192 mM glycine 0,1% SDS

Transfer buffer Co-IP

25 mM Tris, 192 mM glycine, 20% methanol

Transfer buffer LC3 proteins

25 mM Tris, 192 mM glycine, 0,01% SDS, 15% methanol

TBS-T

Tris buffered saline, 0.1% Tween 20

Lysis buffer

150 mM NaCl, 50 mM Tris-HCl, pH 7.4, 1 mM EDTA, 1.0% TritonX-100

Wash buffer

0,1% TritonX-100, 150 mM NaCl, 50 mM Tris-HCl, pH 7.4, 1 mM EDTA

Stripping buffer

6M guanidium HCl, 0,2% TritonX-100, 20mM Tris-HCl pH7,5, 0,1M β-mercaotpethanol

Confocal buffers

Blocking Buffer

5% normal goat serum, 0.3% Triton X-100 in PBS

Antibody Dilution Buffer

1% BSA, 0.3% Triton X-100 in PBS